

DELFT UNIVERSITY OF TECHNOLOGY

Faculty of Electrical Engineering

Telecommunications and Traffic Control Systems group

Title: Development and testing of the airborne part of the MLS Integrated Approach System (MIAS)

Author: R.C. Meijer

Code: A481

Date: March 1993

Abstract: The airborne part of the MLS Integrated Approach System (MIAS) was designed and implemented.

keywords: MLS, DGPS, DME, MLS Integrated Approach System (MIAS),  
Integrated Navigation

## **Preface**

The report that lies in front you, is the result of the effort of the author to get his Masters degree. The information in this report is however not the result of his work alone. At the Telecommunications and Traffic Control Systems group a varying group of students has been working on the MIAS project. The members of this group all researched parts of MIAS in detail. My job was to put those pieces together to form the airborne part of MIAS. Without their co-operation and good-fellowship it would have been much harder for me to complete this job. Of course I should not forget the professional help from the technical staff. I would also like to thank my mentor Edward and professor van Willigen for their support and friendly co-operation.

Hopefully the efforts made to create MIAS will some day result in air traffic which is even safer as it is now.

# Contents

Preface .....	-ii-
Contents .....	-iii-
Summary .....	-vi-
Abbreviations .....	-vii-
Introduction .....	-1-
Part I: MIAS system description .....	-2-
1 MIAS system components .....	-2-
1.1 Microwave Landing System (MLS) .....	-2-
1.2 Differential Global Positioning System (DGPS) .....	-3-
1.3 Inertial Reference System (IRS) .....	-3-
1.4 Distance Measuring Equipment / Precision (DME/P) .....	-4-
1.5 Airborne equipment .....	-4-
1.6 Ground based equipment .....	-5-
2 Positioning .....	-6-
2.1 MLS and GPS positioning .....	-6-
2.2 Hybrid positioning .....	-8-
2.3 Solving the hybrid set of equations .....	-9-
2.4 Roll, pitch and heading for position calculation .....	-11-
3 Accuracy and Integrity .....	-13-
3.1 MIAS Accuracy .....	-13-
3.2 Accuracy determination .....	-15-
3.3 Performance of MIAS as function of ADW channel load .....	-15-
3.3.1 Influence of DGPS on MIAS accuracy .....	-16-
3.3.2 Accuracy as function of the ADW channel load .....	-17-
3.3.3 Example of MIAS accuracy and ADW load .....	-18-
3.4 Sampling of MIAS sensors .....	-19-
3.4.1 Sampling rates in MIAS .....	-19-
3.4.2 Solutions to handle asynchronous samples .....	-20-
3.5 Integrity .....	-21-

3.5.1	Detection	-22-
3.5.2	Identification	-23-
4	Operational Use	-25-
4.1	Advantages and limitations	-25-
4.2	Suggestions for the operational use of MIAS	-25-
4.2.1	MIAS in General Aviation	-26-
4.2.2	MIAS in Air Transport	-27-
4.3	Possible expansions	-27-
Part II:	Testing by Delft University of Technology	-29-
1	Introduction	-29-
2	Hardware and software	-30-
2.1	MIAS hardware	-30-
2.1.1	The test aircraft: the DHC Beaver	-30-
2.1.2	The MLS receiver: Bendix MLS 20-A	-31-
2.1.3	The GPS receiver: Magnavox MX4200D	-32-
2.1.4	The IRS	-33-
2.1.5	The MIAS computer: IBM compatible 486 PC	-34-
2.2	MIAS software philosophy and hierarchy	-34-
3	Test setup	-37-
3.1	Simulation of MIAS	-37-
3.2	MIAS static testing at Schiphol Airport	-38-
3.3	Flight data collection with the DHC Beaver aircraft	-39-
3.4	Suggestions for post-flight	-39-
3.4.1	Structure of the post flight test program	-39-
3.4.2	The DGPS message post processing routine	-40-
3.4.3	The MIAS post processing routine	-41-
3.4.4	Comparing the MIAS position to the Truth reference	-41-
	Conclusions and recommendations	-42-
	Literature	-44-
	Appendix A MLS time multiplex and data words	-47-
	Appendix B GPS timing and errors in pseudo ranges	-52-

Appendix C Errors caused by asynchronicity of information ..... -65-

Appendix D The metric error caused by an angular error ..... -69-

Appendix E MAGNAVOX MX4200D messages for MIAS ..... -71-

Appendix F Bendix MLS 20-A connections to CDU and MIAS computer ..... -77-

Appendix G The ARINC 429 protocol ..... -84-

Appendix H Converting synchro signals to digital words ..... -87-

## Summary

The civil aviation community is executing a transition from the Instrument Landing System (ILS) to the new landing system called Microwave Landing System (MLS). To increase the integrity of landing systems, the MLS Integrated Approach System (MIAS) is proposed. MIAS uses MLS, Distance Measuring Equipment (DME), the Differential Global Positioning System (DGPS) and an Inertial Reference System (IRS). The DGPS messages are transmitted using the MLS Auxiliary Data Word (ADW) channel. MIAS is able to detect erroneous measurements. This property enlarges the safety of the aircrafts landing with MIAS. The aim of MIAS is to provide at least the same accuracy as MLS with a higher integrity. The aim of this report is to design the airborne part of MIAS, to implement an experimental MIAS airborne part and to test it.

In this report, system consideration for the MIAS airborne part are discussed. To evaluate the performance of MIAS, simulations should be run and flight tests be executed. Therefore the design of an interface for the GPS and MLS receivers and an IRS with a computer is described.

As a result of this thesis work, software and hardware are now available for the experimental airborne part of MIAS. This software is easily expandable, which enables different types of equipment to be attached. The expansibility enables also the use of additional positioning sensors. The MIAS experimental airborne equipment could not be evaluated thoroughly yet. Therefore, it is recommended to test the MIAS experimental airborne system more using post processing of flight data and simulations. Post processing and simulation software should be developed for that purpose. Further research should be done into estimation of asynchronous inputs and DGPS algorithms. It is recommended that implementation of additional positioning sensors is researched.

## Abbreviations

ADW	Auxiliary Data Words
AT	Air Transport
ATC	Air Traffic Control
BDW	Basic Data Word
CDOP	Centre line Dilution Of Precision
CG	Centre of Gravity
Det	Detection
DGPS	Differential GPS
DH	Decision Height
DME/P	Distance Measuring Equipment, Precision
DoD	Department of Defense (U.S.)
DPSK	Differential Phase Shift Keying
ECEF	Earth Centred Earth Fixed
EIA	Electronic Industries Association
FA	False Alarm
FCC	Flight Control Computer
FSK	Frequency Shift Keying
GPS	Global Positioning System
HDOP	Horizontal Dilution Of Position
HOW	Hand-Over Word
ICAO	International Civil Aviation Organisation
ILS	Instrument Landing System
IRS	Inertial Reference System
MD	Missed Detection
MIAS	MLS Integrated Approach System
MLS	Microwave Landing System
NAV	Navigation system
NM	Nautical Miles, 1 NM = 1852 meter
NMEA	National Maritime Electronics Association
NO	Normal Operation
OSI	Open Systems Interconnection
PPS	Precise Positioning Service
PRN	Pseudo Random Noise
RAIM	Receiver Autonomous Integrity Monitoring
RVR	Runway Visual Range

SA	Selective Availability
SPS	Standard Positioning Service
TOW	Time of Week
WGS-84	World Geodetic System 1984
X1 epoch	All ones epoch

## Introduction

This report describes a new integrated approach and landing system for aircrafts called the MLS Integrated Approach System (MIAS). An approach system calculates the position of an aircraft during the approach and landing of that aircraft from Initial Approach to Flare. Because landing an aircraft should be done smoothly, it is important to know the position of the aircraft with a high accuracy. In order to develop a landing system with a high safety, it is important to be able to monitor the accuracy of the landing system. If the accuracy gets worse, the pilot should be warned in time. This is called integrity.

The horizontal accuracy of a modern approach system at the threshold is 6 m (95 %) across the runway and 30 m (95 %) along the runway centre line. The vertical accuracy is 60 cm (95 %). If the error in the measurements gets worse than the allowed error, the pilot should be warned within one second. The probability that the pilot is not warned while the errors are too large is required to be  $10^{-9}$  per landing for the whole positioning system. On the other hand, the probability of a false alarm should be kept low,  $0.5 \cdot 10^{-3}$  per landing, because the pilot might eventually ignore the alarms. These numbers are specified by the International Civil Aviation Organisation (ICAO) for the Microwave Landing System (MLS) in [2, sec. 3.11 and table C5] and determine the safety of the landing system.

The aim of MIAS is to provide the same accuracy as MLS with a better integrity. The aim of this report is to design and implement the airborne part of a MIAS experimental system and to evaluate it.

This report is divided in two parts. The first part of the report treats the MIAS system. It starts with discussing the components of MIAS and the problems that arise when integrating these independent components. Then integrated positioning is discussed, followed by a section about accuracy and integrity. The first part of this report ends with suggestions for operational use of MIAS and its pro's and cons.

The second part of this report describes the testing of MIAS. The introduction discusses considerations for the flight tests. Then the hardware and software which will be used for the testing is discussed. The second part ends with the test setup.

Following the two parts, the conclusions are presented. The appendices treat several subjects in more detail.

# Part I: MIAS system description

## 1 MIAS system components

MIAS is an integrated approach system based on MLS, the Differential Global Positioning System (DGPS) and an Inertial Reference System (IRS). It has the possibility to be expanded with Distance Measuring Equipment / Precision (DME/P). Expanding MIAS with DME/P will increase the integrity of the system, thus the safety. The MLS data channel is used to transmit DGPS messages. The accuracy, at the runway threshold, of MIAS is at least the same as of MLS, but the integrity is better, because MIAS uses several independent systems: MLS, DME and DGPS. MIAS uses the MLS azimuth and elevation angle measurements, the DGPS range measurements (and possibly the DME/P distance measurements) to calculate the position of the aircraft. The IRS outputs the attitude angles of the aircraft which are used to adjust the measurements of the different antenna's to a desired point on the aircraft.

The systems described above are connected to the MIAS computer, which reads the information from the MLS receiver, the GPS receiver, the IRS and possibly the DME/P interrogator.

In the following sections, the different components of MIAS are described followed by a summary of the equipment needed for the operational use of MIAS.

### *1.1 Microwave Landing System (MLS)*

The MLS azimuth transmitter sweeps a beam of radio waves in the horizontal plane with a constant angular velocity from one side of the coverage to the other side of the coverage. This beam is wide in the vertical plane and narrow in the horizontal plane. The MLS receiver detects when the beam hits on the aircraft. By dividing the time between the hits on the aircraft by the angular velocity, the azimuth angle of the aircraft referenced to the runway centre line is calculated.

After the azimuth transmitter has finished its sweep, the elevation transmitter does the same as the azimuth transmitter on the same frequency, but now in the vertical plane with a beam wide in the horizontal plane and narrow in the vertical plane. The MLS azimuth transmitter also has a data transmitter which transmits Basic Data Words (BDW's) and Auxiliary Data Words (ADW's). The BDW's and ADW's are used by MLS to transmit integrity messages, the positions of the MLS transmitters, etc. MIAS uses ADW's to transmit DGPS messages. More information about MLS can be found in appendix A and [2, sec. 3.11].

## *1.2 Differential Global Positioning System (DGPS)*

The ranges from the aircraft to one of the Global Positioning System (GPS) satellites are calculated by dividing the travel time of radio signals by their speed. GPS satellites modulate a 50 bit per second data stream on a 1575 MHz carrier, which contains parameters to calculate the satellite positions and the time of the transmissions. The formulas for calculating the satellite position are listed in appendix B and in [3]. By subtracting the transmission time from the reception time, the travel time is calculated. The reception time is determined by a receiver clock in the aircraft which is not synchronous with the satellite clocks. This causes a clock offset, which can be calculated by using at least four measurements for 3-D positioning or three measurements for 2-D positioning. The horizontal positioning accuracy of the Standard Positioning Service (SPS) is 100 m (95 %), [3, page A-4]. This number is calculated using an accuracy of 30 m (95 %) for the range measurements, assuming a Horizontal Dilution of Precision (HDOP) of 1.7. The range accuracy can be improved by using a reference station at a known location, which calculates the errors in the GPS range measurements and transmits the errors as DGPS messages to the aircraft. In MIAS these DGPS messages are transmitted using the MLS ADW's.

## *1.3 Inertial Reference System (IRS)*

The IRS measures the attitude of the aircraft. The attitude of the aircraft is determined by the roll, the pitch and the heading of the aircraft. The roll angle is the angle of the aircraft around the along axis the aircraft, which is zero when the wings of the aircraft are level with the horizon. The angle around the cross axis is called the pitch angle, which is also zero when the aircraft is level with the horizon. The angle of the aircraft around the top axis is called the heading angle. The heading is zero when the along axis points North. This is True North.

There are different ways to measure the attitude of an aircraft. The most simple way is to use two gyro's which are slaved by the earth's gravitation and the earth's magnetic field respectively. More modern strap down inertial reference systems use accelerometers to calculate the attitude of the aircraft. Non-inertial ring laser gyroscopes determine the attitude of the aircraft using the effects of rotation of electromagnetic waves. More information about these methods of determining the attitude of the aircraft can be found in [1].

For MIAS, it is not important how the attitude angles (pitch, roll and heading) are measured. The position error of MIAS consists of the errors in the MLS, GPS, DME and the attitude measurements. The error in the attitude (in radians) adds up to the resultant of the MLS, GPS and DME errors. This is explained in appendix D.

### *1.4 Distance Measuring Equipment / Precision (DME/P)*

To determine the distance of the aircraft to a DME/P ground station, the so-called DME/P interrogator in the aircraft transmits a pair of pulses. These pulses travel with a certain speed to the DME/P ground station, which receives the pulses, holds them and transmits them again. As soon as the DME/P interrogator in the aircraft receives the pulses again, it can calculate the distance to the DME/P ground station by dividing the travel time by the speed of the radio signals. The DME is described in detail in [1] and in [2].

### *1.5 Airborne equipment*

As was mentioned above, for MIAS a MLS and GPS receiver and associated antenna's are needed. The MLS receiver should be able to receive and output the azimuth and elevation angles and the data functions in a format readable for the MIAS computer. The GPS receiver should output pseudo ranges and the GPS message for the calculation of the satellite positions. As discussed in the previous section, the roll, pitch and heading of the aircraft should be measured also. These angles are output by the IRS. If higher integrity is needed, a DME/P interrogator and antenna is needed and should be installed in the aircraft. Furthermore a MIAS computer is needed, which can be connected to each of these devices.

### 1.6 Ground based equipment

The equipment for the ground based part of MIAS consists of a MLS azimuth and elevation transmitter and associated monitors and the MLS data transmitter, which is located at the azimuth transmitter. This data transmitter should be able to accept and transmit ADW's which are offered by an external source. For MIAS, a DGPS reference station is needed. This station consists of a multi channel GPS receiver with antenna and a computer which calculates the GPS corrections and forms ADW's. Finally a data connection is needed between the DGPS reference station and the MLS data transmitter. If higher integrity is needed, a DME/P ground station with associated monitor should be installed.

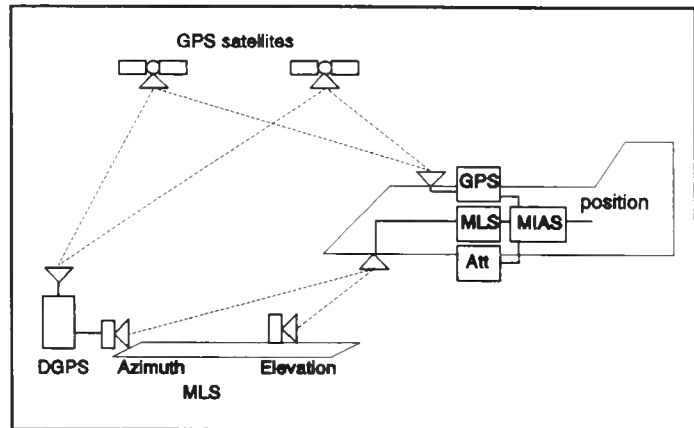


Figure 1.1 Overview of the MIAS ground and airborne equipment.

The resulting MIAS system is sketched in figure 1.1.

## 2 Positioning

This section will describe the hybrid positioning method used in MIAS which assures that all MLS angles, GPS ranges, IRS angles and possibly DME/P distances available are used. Hybrid positioning also opens opportunities to check the validity of the calculated position. Before describing the hybrid position solution, positioning with only MLS or GPS is described shortly. This section ends with an explanation of how the attitude information of the aircraft is used.

### 2.1 MLS and GPS positioning

The MLS position of the aircraft can be determined with the azimuth and elevation angle measurements and the DME/P distance measurement. The azimuth angle defines a vertical plane in which both the azimuth transmitter and the MLS receiver are located. The elevation angle defines another plane with an angle to the horizon in which both the elevation transmitter and the MLS receiver are located. The

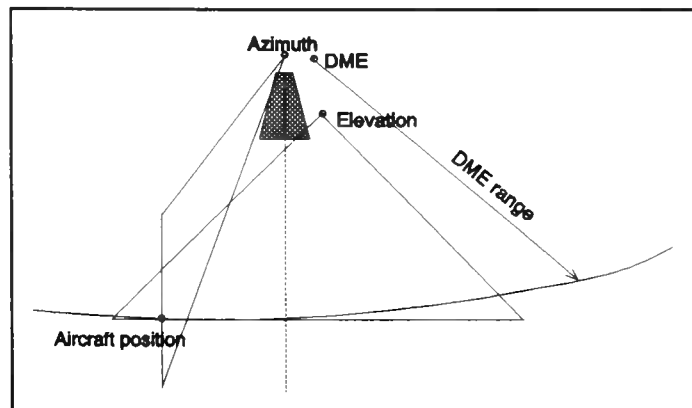


Figure 2.1 MLS positioning with azimuth, elevation and DME.

The intersection of the elevation plane and the azimuth-plane forms a line on which the MLS receiver is located. The DME/P distance measurement determines a sphere. By intersecting the sphere and the azimuth-elevation line, the position of the MLS receiver is determined. This is illustrated in figure 2.1.

The relations between the MLS azimuth and elevation measurements and the MLS antenna position can be derived using figure 2.2 and 2.3 for planar scanning beams.

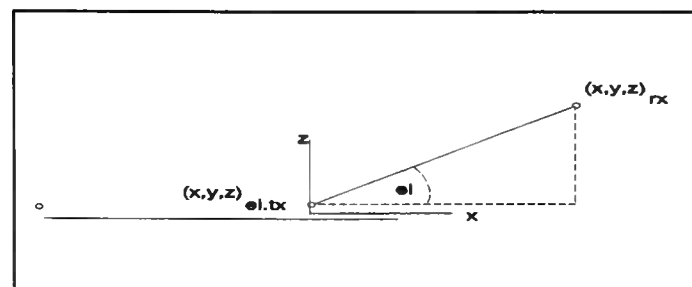


Figure 2.2 The relation between the elevation angle, the MLS antenna position and the MLS elevation transmitter position.

Formulas (2.1) and (2.2) show the results.

$$az = \text{atan} \left( \frac{y_{rx} - y_{az.tx}}{x_{rx} - x_{az.tx}} \right) \quad (2.1)$$

$$el = \text{atan} \left( \frac{z_{rx} - z_{el.tx}}{x_{rx}} \right) \quad (2.2)$$

The equations for conical scanning beams are more complicated and won't be treated here. The equations for conical scanning beams can be found in [14] and [24]. Note that the equations are for a local reference system.

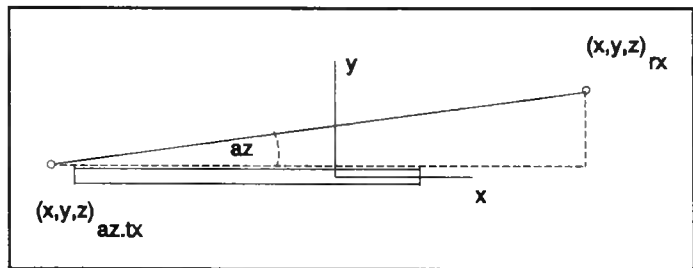


Figure 2.3 The relation between the azimuth angle, the MLS antenna position and the MLS azimuth transmitter position.

The DME/P equation is derived using figure 2.4. Formula (2.3) shows the equation which relates the DME/P interrogator position to the DME/P ground station location and the distance measurement.

$$\sqrt{(x_{interro} - x_{ground})^2 + (y_{interro} - y_{ground})^2 + (z_{interro} - z_{ground})^2} = D \quad (2.3)$$

Note that three independent measurements are required: azimuth, elevation and distance, to determine the MLS receiver position in 3-D.

Each GPS satellite transmits a continuous radio signal which is modulated by a bit stream and a unique Pseudo Random Noise (PRN) code. The PRN code enables the GPS satellites to transmit all at the same frequency. The bit stream contains parameters for the GPS satellite

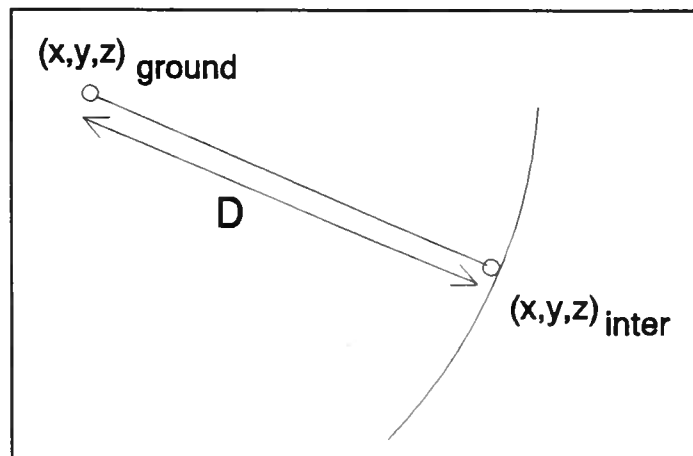


Figure 2.4 The relation between the DME distance measurement and the position of the DME interrogator and the DME ground station.

position calculation<sup>1</sup>. From the information in the bit stream and the chips in the PRN code, the time of transmission of each chip in the PRN code can be determined. If the time of transmission of the chip in the PRN code is subtracted from the reception time of the chip, the travel time of the radio signal is determined. Multiplying the travel time with the speed of radio signals results in the distance between the GPS satellite and the GPS receiver.

The timer in the GPS receiver is not synchronous with the timer in the GPS satellites, which results in an offset in the travel time. This offset is equal for all range measurements, because the GPS satellites are synchronised among themselves. Because of the common offset, the measured ranges to the GPS satellites are called pseudo ranges. The position of the GPS receiver and the clock offset can be determined using at

least four GPS pseudo ranges. The pseudo ranges form spheres around the GPS satellites. The intersection of the four spheres determines the GPS receiver position. This is illustrated in figure 2.5. More information about GPS can be found in appendix B and [10] and [3].

Note that it takes four pseudo ranges to determine the 3-D position of the GPS receiver.

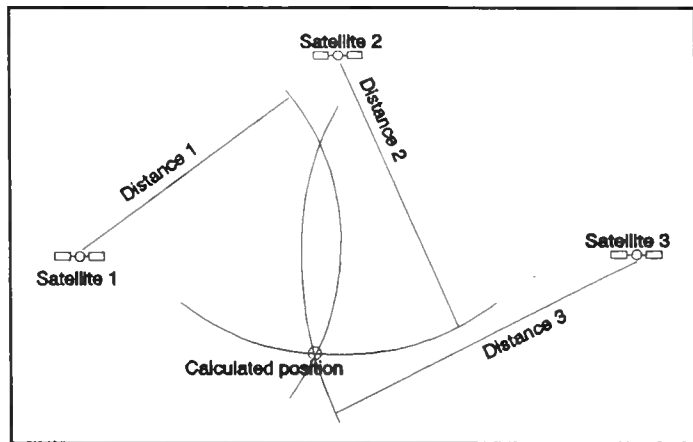


Figure 2.5 GPS positioning with pseudo ranges.

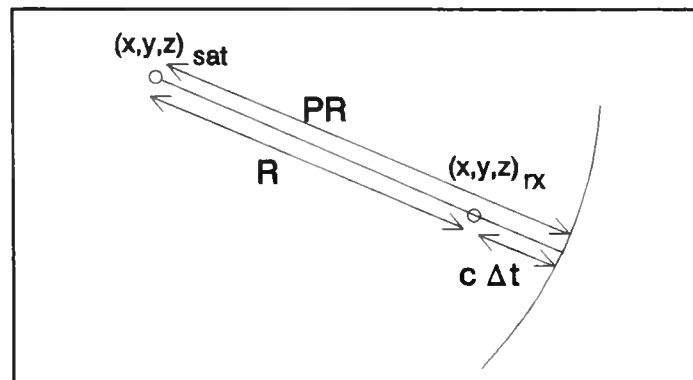


Figure 2.6 The relation between the GPS measurement and the position of the GPS antenna and the position of the GPS satellite.

<sup>1</sup> Appendix B lists all necessary formulas.

With figure 2.6, the equation for the GPS measurements, as shown in (2.4), follows.

$$\sqrt{(x_{rx}-x_{sat})^2 + (y_{rx}-y_{sat})^2 + (z_{rx}-z_{sat})^2} + c \cdot \Delta t = PR \quad (2.4)$$

The GPS satellite position is calculated in the WGS-84<sup>1</sup> reference system, which is different from the local reference system used for MLS. To be able to use both measurements, the WGS-84 position of the origin of the local reference system should be known. Positions in one reference system can then be converted to positions in the other reference system.

## 2.2 Hybrid positioning

The output of a positioning system is an estimate of the actual position. Outputs of two or more positioning systems can be combined to make another estimate of the actual position. This is called 'Integrated positioning', [26, sec.8]. If GPS and MLS are combined in an integrated manner, both systems need to provide a full position estimate. Another way of combining GPS and MLS has more advantages. This way is called 'Hybrid positioning', [26, sec.8].

The hybrid positioning in MIAS uses the MLS azimuth, and elevation angle, GPS pseudo ranges to the satellites and possibly the DME/P distance measurement. With these pieces of information, a set of equations can be formed which describes the relations between the measurements and the position of the receiver. These equations are used to solve the set of unknown parameters : X, Y, Z and the user clock error of the GPS receiver  $\Delta t$ . The minimum set of equations contains as many equations as the number of measurements available. So if for example MLS azimuth and elevation are measured plus two GPS-ranges, the number of unknowns will be four and the number of equation will be four as well. Because the number of unknowns is then equal to the number of equations and the equations are independent, this set can be solved uniquely.

Note that in the example neither MLS nor GPS would be able to determine the position of the aircraft by itself. However, using the hybrid positioning method, it is possible to determine the position.

---

<sup>1</sup> World Geodetic System 1984. This is a Earth Centred Earth Fixed (ECEF) system. More information about WGS-84 can be found in [10].

### 2.3 Solving the hybrid set of equations

The equations from the previous section are non-linear, which makes them difficult to solve analytically. By linearising these equations, they can be handled better. Differentiating the equations at a point  $(X, Y, Z, \Delta T)$  gives a linear set of equations which can be solved with the measurements. The results give  $dX$ ,  $dY$ ,  $dZ$  (and  $dT$  if GPS is used). If these numbers are added to the starting point  $(X, Y, Z, \Delta T)$ , a new estimate of the position results. This iteration process can be repeated until the difference between two estimated positions is small enough. This is shown in figure 2.7.

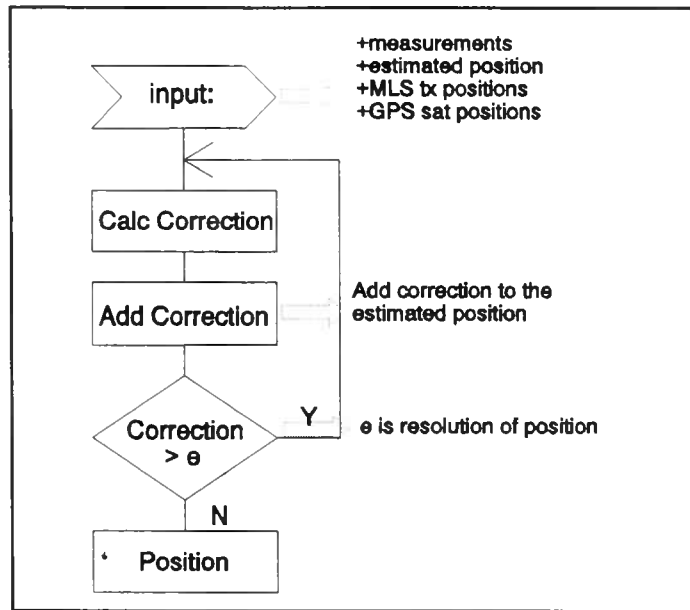


Figure 2.7 Flow chart illustrating the iterative calculation of the position.

The linearised equations for MIAS, using GPS and MLS azimuth and elevation and DME distance, can be written as in (2.5). They are derived in [14]. Note that the MLS equations used here are the linearised equations for the conical scanning beams.

$$\begin{bmatrix}
 \frac{(x^{est}-x_1)}{R_1^{est}} & \frac{(y^{est}-y_1)}{R_1^{est}} & \frac{(z^{est}-z_1)}{R_1^{est}} & c \\
 \frac{(x^{est}-x_2)}{R_2^{est}} & \frac{(y^{est}-y_2)}{R_2^{est}} & \frac{(z^{est}-z_2)}{R_2^{est}} & c \\
 \dots & \dots & \dots & \dots \\
 \frac{(x^{est}-x_i)}{R_i^{est}} & \frac{(y^{est}-y_i)}{R_i^{est}} & \frac{(z^{est}-z_i)}{R_i^{est}} & c \\
 -\frac{\sin(\alpha^{est})\cos(\alpha')}{R_\alpha} & -\frac{\cos(\alpha^{est})}{R_\alpha} & -\frac{\sin(\alpha^{est})\cos(\alpha')}{R_\alpha} & 0 \\
 -\frac{\sin(\theta^{est})\cos(\theta')}{R_\theta} & \frac{\sin(\theta^{est})\sin(\theta')}{R_\theta} & \frac{\cos(\theta^{est})}{R_\theta} & 0 \\
 \cos(\beta)\cos(\beta') & \cos(\beta)\sin(\beta') & \sin(\beta) & 0
 \end{bmatrix} \cdot \begin{bmatrix} dX \\ dY \\ dZ \\ dT \end{bmatrix} = \begin{bmatrix} R_1^{meas} - R_1^{est} \\ R_2^{meas} - R_2^{est} \\ \dots \\ R_i^{meas} - R_i^{est} \\ \alpha^{meas} - \alpha^{est} \\ \theta^{meas} - \theta^{est} \\ R_{DME}^{meas} - R_{DME}^{est} \end{bmatrix} \quad (2.5)$$

The linearised set of equations can be written as a general matrix-equation, which is shown in (2.6)

$$A \cdot \underline{u} = \underline{v} \quad (2.6)$$

Where 'A' is the matrix with the known parameters like the satellite position, an estimate of the user position etc. 'u' is the vector with the unknown adjustments (dX, dY, dZ, dT) to the starting position (X,Y,Z,ΔT) and 'v' is the difference vector of the measurements and estimated angles and ranges. If 'A' is square, which means that there are as many equations as unknowns, 'u' can be solved as shown in (2.7).

$$\underline{u} = A^{-1} \cdot \underline{v} \quad (2.7)$$

A non-square matrix can be made square by multiplying it with its transpose. This is exactly what the Least Squares Error (LSE) method does, to calculate the best estimate of the position in case there are more equations than unknowns. Formula (2.8) shows the LSE method to solve 'u'.

$$\underline{u} = (A^T A)^{-1} A^T \cdot \underline{v} \quad (2.8)$$

The formulas above only treat the case where each measurement has the same weight. However, if the aircraft is close to the runway, the MLS elevation accuracy will be much better than the DGPS range accuracy. To make the most accurate measurements more important in the position calculation, a weight matrix 'W' is introduced. It is a diagonal-matrix with on its diagonal for every measurement a number. The bigger the number the more influence the measurement has on the

position. The Weighed LSE method replaces 'A' with 'WA' and 'y' by 'Wy'. This results in formula (2.9)

$$\underline{u} = (A^T W^T W A)^{-1} A^T W^T W \cdot \underline{y} \quad (2.9)$$

Where 'W<sup>T</sup>W' is the inverse of the covariance matrix 'C' of the measurements.

More information about the LSE and Weighed LSE method can be found in [21, section 3] and [14].

### 2.4 Roll, pitch and heading for position calculation

Because of Cat III accuracy criteria for landing aircrafts, see [2, sec 3.1], the position of an aircraft is to be determined with an accuracy of decimeters.

Calculating the position with the 'raw' measurements of MLS, GPS and DME will result in a position of an undefined point on the aircraft somewhere between the MLS, GPS and DME antenna, because MLS, GPS and DME use different antenna's. The MLS, GPS and DME measurements should be adjusted to take their different positions into

account, see figure 2.8. For GPS and DME the adjustment will be the addition of a vector to each range measurement. The vector has a length equal to the distance between the GPS antenna (or DME antenna) and a virtual antenna and an orientation dependent on the attitude of the aircraft. For MLS the adjustment will be the addition of an angle to the azimuth and elevation measurements. The size of the angle to be added is dependent on the attitude of aircraft but also on the location of the aircraft and the azimuth and elevation transmitter positions. The dependence on the aircraft and azimuth and elevation transmitter positions makes the MLS adjustment more complex to calculate than the GPS or DME adjustment.

The location of the virtual antenna can be anywhere on the aircraft. By picking a clever point on the aircraft, only one of the subsystem measurements needs to be adjusted. By taking for example the MLS antenna as the virtual antenna point, only the GPS measurements need to be adjusted, which is simpler than adjusting the MLS measurements to the GPS antenna. This argument holds only for aircrafts with one MLS antenna. For aircrafts with more MLS antenna's the virtual antenna position should be at a point where the distance to all MLS, GPS and DME antenna's is shortest. The longer

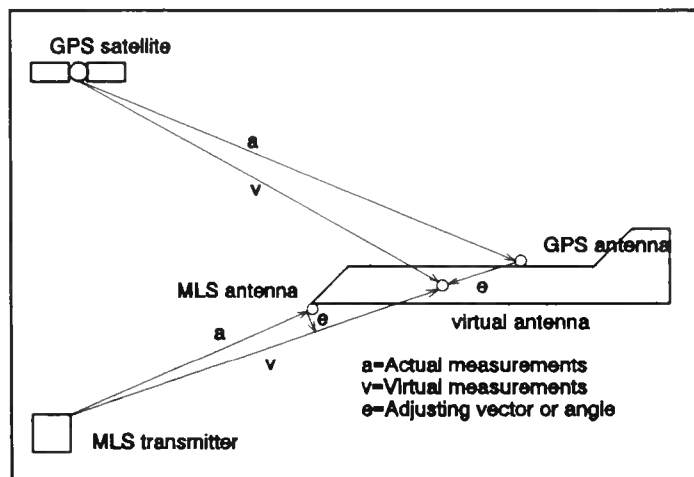


Figure 2.8 Calculation of the virtual antenna position with MLS and GPS.

the distance between the virtual antenna and a real antenna, the greater the influence of an attitude angle error.

By adding a vector to this virtual antenna point, the position of the desired point can be calculated. During the flare of a landing, the pilot is mostly interested in the position of the main landing gear.

During the Initial Approach, he is more

interested in the Centre-of-Gravity (CG) of the aircraft, because the aircraft rotates around the CG. Anyway, a vector to one of these points needs to be added to the virtual antenna point.

The orientation of the GPS adjustment vector and the CG vector can be calculated by using the roll, pitch and heading angles of the aircraft. An example to illustrate the attitude dependence of the vector to the landing gear is given in figure 2.9 for an aircraft with a pitch angle. The formula for the transformation of vectors is given in (2.10),

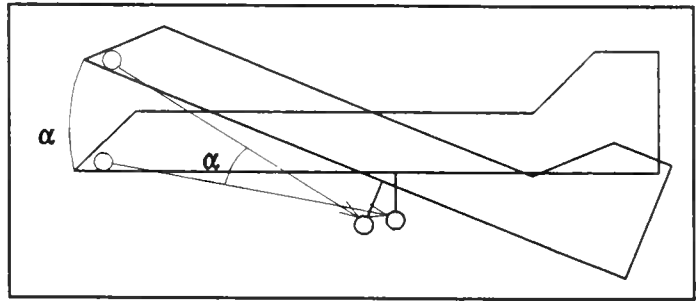


Figure 2.9 The desired point is calculated by adding a rotated vector to the virtual-antenna.

$$\begin{bmatrix} U_x(\phi, \theta, \psi) \\ U_y(\phi, \theta, \psi) \\ U_z(\phi, \theta, \psi) \end{bmatrix} = \begin{bmatrix} 1 & 0 & 0 \\ 0 & \cos(\phi) & \sin(\phi) \\ 0 & -\sin(\phi) & \cos(\phi) \end{bmatrix} \cdot \begin{bmatrix} \cos(\theta) & 0 & \sin(\theta) \\ 0 & 1 & 0 \\ -\sin(\theta) & 0 & \cos(\theta) \end{bmatrix} \cdot \begin{bmatrix} \cos(\psi) & \sin(\psi) & 0 \\ -\sin(\psi) & \cos(\psi) & 0 \\ 0 & 0 & 1 \end{bmatrix} \cdot \begin{bmatrix} U_x(0,0,0) \\ U_y(0,0,0) \\ U_z(0,0,0) \end{bmatrix} \quad (2.10)$$

where  $U(0,0,0)$  is the vector at zero attitude and  $U(\phi, \theta, \psi)$  is the vector after the transformation. ' $\phi$ ' is the roll angle around the along axis, which points through the nose of the aircraft, ' $\theta$ ' is the pitch angle around the across axis, which points in the direction of the right wing and ' $\psi$ ' is the heading around the top axis which points down. The adjustment of GPS measurements and the transformations are extensively described in [14].

### 3 Accuracy and Integrity

This section discusses the accuracy of the MIAS position calculation and its dependence on the DGPS accuracy and DGPS update rate. Further more, a way to determine the accuracy of the MIAS position is discussed. Following that the problem of asynchronous information is discussed. Conclusively the integrity of MIAS is examined.

#### 3.1 MIAS Accuracy

The accuracy of MIAS depends on the accuracy of each of the measurements and the geometry of the measurements. The influence of the geometry is determined by the transmitter positions, the aircraft position and the kind of measurement taken. For example in figure 3.1, the range measurement 'R' is accurate along the line through the azimuth transmitter and the aircraft, while the angle measurement 'azimuth' is accurate perpendicular to that line.

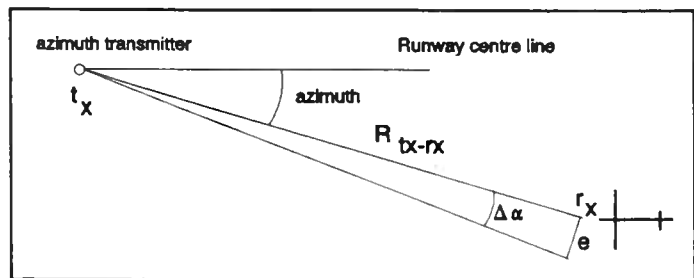


Figure 3.1 The metric error due to the azimuth angular error.

The accuracy of the measurements varies as function of the position. For example: the MLS angle measurements have a fixed angular error, but their metric error will increase with the distance from the transmitters as can be seen from figure 3.1 and formula (3.1).

$$e = R_{tx-rx} \cdot 2 \cdot \sin \left( \frac{1}{2} \Delta \alpha \right) \quad (3.1)$$

Where ' $R_{tx-rx}$ ' is the distance between the azimuth transmitter and the MLS antenna, ' $\Delta \alpha$ ' is the azimuth angular error and 'e' is the metric error caused by the angular error. The MLS azimuth and elevation angular error are not defined, but can be calculated from the allowable metric error at the threshold and the distance between the azimuth or elevation transmitter and the threshold. The azimuth angular error is then:

$$\Delta \alpha = 2 \cdot \arcsin \left( \frac{1}{2} \frac{e_a}{R_{tx-thres}} \right) \quad (3.2)$$

Where ' $\Delta \alpha$ ' is the azimuth angular error, ' $e_a$ ' is the allowable metric error at the threshold caused by the azimuth measurement and ' $R_{tx-thres}$ ' is the distance between the threshold and the azimuth transmitter. For calculating the elevation angular error formula (3.2) can be used again. In that case

' $\Delta\alpha$ ' is the elevation angular error, ' $e_a$ ' is the allowable metric error at the threshold caused by the elevation measurement and ' $R_{\text{tx-thres}}$ ' is the distance between the elevation transmitter and the threshold. If existing recommendations about siting, [2, Att G, sec 4], are used, MLS multipath won't cause trouble.

The accuracy of the GPS range measurements is dependent on the position of the GPS receiver antenna on earth and the positions of the satellites tracked. Satellites at a low elevation angle will have a worse accuracy than satellites at a higher elevation. The GPS range measurements will have an accuracy of 30 m (95 %). The GPS accuracy improves very much in the MLS coverage, because the DGPS messages can be received there. Within the MLS coverage volume, the DGPS accuracy will be almost constant at a certain instant, because the distance of the GPS antenna to the GPS satellites is approximately the same within the MLS coverage. GPS multipath can still ruin the measurements. The multipath can be minimised by carefully positioning the GPS antenna on the aircraft and using the integrity routines to identify multipath infected measurements. The speed of the aircraft in some cases induces a scalloping rate so high, that the multipath error can be filtered out.

The accuracy of the DME/P changes during the approach. First the DME/P operates in Initial Approach (IA) mode and has an accuracy of 250 m (95 %), at a distance of 7-8 NM, the DME/P interrogator switches over to the Final Approach (FA) mode and has an accuracy of 30 m (95 %), [2].

The accuracy of the attitude information depends very much on the type of IRS used to measure the attitude. The allowable error caused by the IRS measurements depends also on the maximum distance of the MLS, GPS and DME/P antenna's to the desired point. The greater the distance the smaller the allowable angular error. As was mentioned above, the position error is linear with the angular error and linear with the antenna to desired point distance.

The resulting accuracy as function of the position around the runway will look like figure 3.2. 'I' is the area outside the MLS coverage. The position accuracy in the horizontal plane in that area is the standard GPS SPS accuracy of 100 m (95 %). The vertical accuracy is 200 m (95 %). Area 'II' is the area inside the MLS coverage where the DGPS accuracy is better than the MLS accuracy. In area 'III' the MLS elevation metric accuracy is better than the DGPS accuracy. The distance 'x' is dependent on the DGPS accuracy, which is dependent on the update rate of the DGPS messages. A fourth area can be defined where the azimuth metric accuracy is better than the DGPS accuracy. This area is usually small.

### 3.2 Accuracy determination

The accuracy of MIAS can be determined by the airborne part by assuming certain errors on the measurements. The errors for GPS measurements will be 30 m (95 %), but for DGPS the error depends on the update rate of the DGPS messages. The error in the MLS angle measurements and the attitude angle measurements will be fixed and expressed in degrees or radians. If the accuracy of the measurements is known, the covariance matrix of these measurements can be calculated. The relation between the covariance of the position accuracy and the covariance of the measurements is given by formula (3.3).

$$\text{cov}(\underline{u}) = \mathbf{A} \cdot \text{cov}(\underline{y}) \cdot \mathbf{A}^T \quad (3.3)$$

Where 'A' is the matrix used to calculate the position, 'y' is the measurement vector and 'u' is the position vector. The numbers on the diagonal of the cov(u) are the accuracies in the X, Y, Z direction and the ΔT accuracy. More information can be found in [8].

### 3.3 Performance of MIAS as function of ADW channel load

This section describes the relation between the MIAS performance and the update rate of the DGPS messages. GPS errors are calculated by the DGPS reference station and send to the MLS data transmitter, which transmits them to the aircraft using ADW's. The DGPS messages consist of the coefficients of a polynomial with the variable time, which approximates the GPS error. The airborne MIAS computer calculates the DGPS corrections as function of time. The ADW channel is already being used for MLS data and will probably be used for Air Traffic Control (ATC) data in the future. Therefore the load needs to be minimized. Minimising the ADW load means less DGPS messages per second, which causes the DGPS accuracy decrease. The DGPS accuracy should however be accurate enough to enable the MIAS position accuracy to meet Cat III accuracy limits.

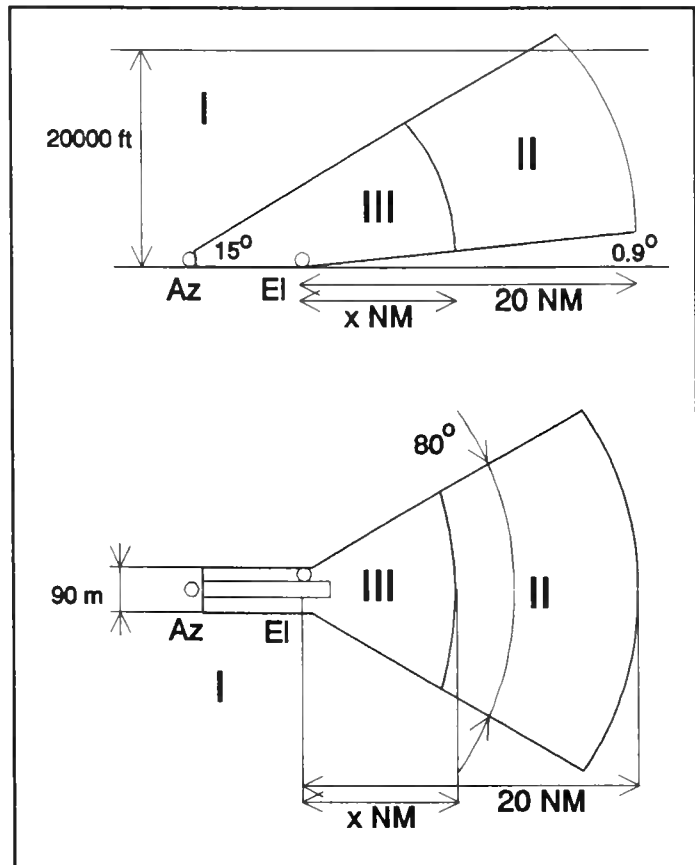


Figure 3.2 The areas with equal error in and outside the MLS coverage.

First the influence of DGPS on the MIAS accuracy is discussed, followed by the accuracy of DGPS as function of the ADW channel load.

### 3.3.1 Influence of DGPS on MIAS accuracy

Outside the MLS coverage, no MLS ADW's can be received, so no DGPS messages can be obtained. MIAS will then be reduced to ordinary GPS. Just within the MLS coverage, coming from the outer boundary, DGPS messages can be received and the position accuracy will improve depending on the accuracy of the GPS corrections. The accuracy of the corrections depends on the age of the corrections, because the GPS errors are mainly caused by Selective Availability (SA), which is a time varying error. The SA error is decorrelated within 200

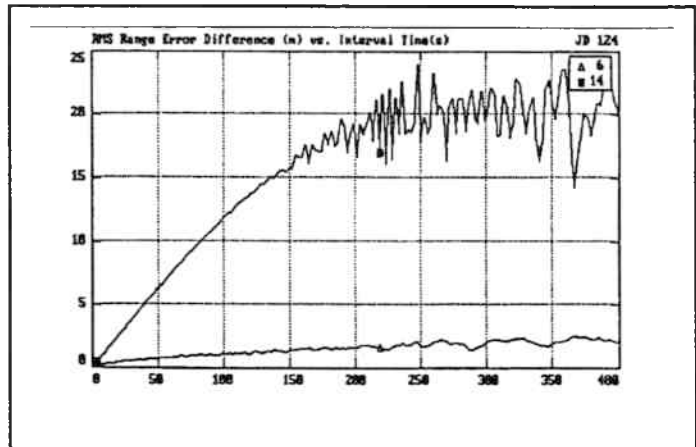


Figure 3.3 DGPS accuracy as function of time. From 'The Effect of Selective Availability on Differential GPS Corrections' by G.T. Kremer, Navigation: Journal of the Institute of Navigation, Vol.37, No. 1, Spring 1990.

seconds. The faster the corrections can be transmitted to the aircraft, the better the GPS measurements can be corrected. Figure 3.3 shows the accuracy of the corrected GPS ranges as function of time. When approaching the runway, beyond a certain point, the MLS elevation angle measurements will become more accurate than the corrected GPS measurements. The MLS azimuth angle measurements will become more accurate than the DGPS measurements at the threshold only if the DGPS accuracy is worse than 6 m (95 %).

The MLS measurements will result in a line of position with a small uncertainty in the azimuth and elevation scanning directions at the threshold. The position on this line of position is not known in the direction radial from the MLS transmitters. If the MLS transmitters are located near the runway, this means that the two smallest dimensions of the error volume are like a plane perpendicular to the runway centre line<sup>1</sup>. The DGPS ranges and the DME/P distance have to provide the accuracy in the direction along the runway centre line. When only considering geometry aspects, the accuracy can best be met using satellites that have a low elevation angle. On the other hand, measurements to satellites at a very low elevation angle will have a worse accuracy compared to

---

<sup>1</sup> The plane is actually perpendicular to the glide path. Since most glide paths are not very steep, only 3 to 6°, the difference is minimal. Using curved approaches, the glide path is less easy to define.

measurements to satellites with a higher elevation angle. A compromise between the improvement of the geometry and the deterioration of accuracy should be made.

Because the position accuracy of MIAS along the runway centre line should be the same<sup>1</sup> as the basic MLS using the DME/P, the position accuracy along the runway centre line needs to be between 12 and 30 m (95 %) depending on the glide slope used<sup>2</sup>. The necessary accuracy of the corrected GPS ranges depends now on the Centre line Dilution Of Precision (CDOP), which relates the corrected GPS range measurements to the GPS accuracy along the runway centre line as shown in formula (3.4).

$$e_{c.l.} = CDOP \cdot e_{range} \quad (3.4)$$

Where ' $e_{c.l.}$ ' is the error along the runway centre line, which is equal to the Along Track Error caused by GPS. In formula (3.4), ' $e_{range}$ ' is the error of a corrected range measurement. The accuracy of the corrected GPS measurements, in its turn, depends on the accuracy of the DGPS messages, which depends on the age of the messages, as was shown before.

The CDOP will be smaller than the Horizontal Dilution Of Precision (HDOP), because the CDOP is only in one horizontal direction, where the HDOP is also in a direction perpendicular to the CDOP. Taking the maximum of all possible HDOP's at the runway location as an estimate of the CDOP is a safe approximation. Information about the way the HDOP is calculated can be found in [10].

To determine the allowable error for the DGPS messages, one has to determine the maximum CDOP for a certain site. It should be the maximum of the CDOP's calculated for all different satellite constellations that can occur. Then the maximum allowable range error can be calculated using formula (3.4). From the maximum range error, the maximum allowable time for the DGPS messages can be found using figure 3.3.

### 3.3.2 Accuracy as function of the ADW channel load

The aim of MIAS is to use the ADW data channel as little as possible, but just enough to achieve the necessary accuracy needed for Cat III landing. This means transmitting as few ADW's per second as possible without compromising on the accuracy. Using as few ADW's as possible has the advantage that other users can send more ADW's per second.

---

<sup>1</sup> It is debatable if the 12 to 30 m (95 %) accuracy is necessary for safe Cat. III landing. The runway is long enough to permit greater error along the runway centre line.

<sup>2</sup> The accuracy of the DME for steep slopes, for STOL or VTOL aircrafts, needs to be higher. Also for Computed Centre Line and curved approaches, the DME accuracy should be better.

In the allowable time, determined in the previous section, the DGPS messages should be calculated by the DGPS reference station and be transmitted to the MLS data transmitter. There the DGPS messages might have to wait in a queue before being transmitted. Also the transmission from the MLS data transmitter to the airborne receiver will contribute to the allowable time. The accumulated time until now is the time from the instant the calculation of the DGPS message started, to the instant the first bit of the message was received by the airborne receiver. Because the complete message needs to be received, the bit rate should be included too. Furthermore the corrections need to be used for some time in the aircraft before a new correction arrives. This can be summarised in formula (3.5).

$$t_{allow} = t_{calc} + t_{ref-MLS_x} + t_{que} + t_{MLS_x-MLS_{rx}} + \frac{bits}{bitrate} + t_{use} \quad (3.5)$$

Note that the bit rate of the MLS data transmitter is 15625 bits per second.

The number of bits transmitted per DGPS message, depends on the number of satellites used to generate DGPS messages and the accuracy of the corrections. The bits transmitted will be packed in ADW's. The packing can be done at the reference station, so the MLS data transmitter only has to queue and transmit ADW packets.

### 3.3.3 Example of MIAS accuracy and ADW load

Suppose the accuracy needed in the direction of the runway centre line is 30 m (95 %) and the maximum possible HDOP at the runway, as an estimate of the CDOP, is 5. Assuming eight satellites being tracked by the reference station, the accuracy of the DGPS measurements, using formula (3.4), should be  $(30 \text{ m} / 5) = 6 \text{ m}$  (95 %). Using the DGPS accuracy curve from figure 3.3 multiplied by 2, to make a worst case calculation, it follows that during 25 seconds the DGPS corrections are accurate enough.

Assume that for each satellite a DGPS message is transmitted consisting of one ADW. This is a conservative assumption, found by experiments. The total amount of transmitted bits from the reference station to the MLS data transmitter is  $8 * 76^1 = 608$  bits at a rate of 10 Kbit per second<sup>2</sup>. The number of bits transmitted by the MLS data transmitter is the same, but with a bit rate of 15625 bits per second. The delay because of transmission is therefore:  $(608 / 10000) + (608 / 15625) = 0.0997$  seconds. This leaves  $25 - 0.0997 \approx 25$  seconds for the DGPS message calculation, the queuing

---

<sup>1</sup> See appendix A for a ADW description.

<sup>2</sup> This bit rate is fictive.

and the use in the aircraft. Assuming 1 second for the calculation and 1 second for the queuing, this leaves 23 seconds for use in the aircraft<sup>1 2</sup>.

The ADW channel load is then 8 ADW's per 25 seconds. Comparing this to the available ADW's per second<sup>3</sup>, 35 ADW's average per second, the MIAS load for this case is 9.14 ‰ which is very small. The available ADW's per second is 35 if the flare and growth slots can be used to transmit BDW's or ADW's. If these slots cannot be used, the available ADW's per second is 16.6, which means that the MIAS load on the ADW channel is 19.27 ‰.

### *3.4 Sampling of MIAS sensors*

In this section, data sampling problems with MIAS are described and solutions for these problems are proposed. First the sampling rates of MIAS and its subsystems are discussed, followed by solutions to handle asynchronous samples.

#### **3.4.1 Sampling rates in MIAS**

All subsystems of MIAS: GPS, MLS, DME/P and attitude sensor, have a different sampling rate. The GPS receiver has a sampling rate depending on the type of receiver and can typically be between 1 and 5 samples per second, the MLS azimuth information comes in at 13 times a second and the MLS elevation information comes in at 39 times a second. The update rate of the attitude information is not specified. The DME/P has a sample rate depending on the mode in which it is operating. The IA mode has a sample rate of 16 samples per second and the FA mode 40 samples per second, [2].

This causes a problem if the MIAS computer wants to calculate a position, because it is not clear which information should be used and at which instant. If worst case is considered for MLS and GPS, the GPS information comes 1/13 of a second after the azimuth information and just 1/39 of a second after the elevation. This is shown in figure 3.4.

---

<sup>1</sup> Some receivers validate ADW's on a majority voting. Constantly changing ADW's will not be accepted by these receivers. These receivers should be adapted or expanded for MIAS use.

<sup>2</sup> These calculations do not account for errors during transmission. The ADW parity will solve some errors.

<sup>3</sup> The available ADW's per second are calculated in Appendix A.

### 3.4.2 Solutions to handle asynchronous samples

There are several ways to handle these asynchronous samples. Two possible solutions are described in this section.

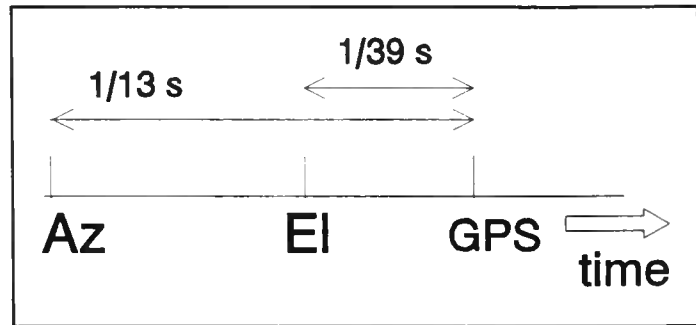


Figure 3.4 Arrival of subsystem information in time.

The first solution is very simple: Every time the slowest information source delivers an information package, the position is calculated, using the most recent information from the other devices. So MIAS calculates a position every time the GPS information is available, because it is the slowest information source. For this position calculation the most recent MLS azimuth and elevation is used.

This process is depicted in figure 3.5 for MLS and GPS. This scheme has the disadvantage of using only very little of the MLS azimuth and elevation information available. Only 1 out of 13 azimuth samples and only 1 out of 39 elevation samples is used<sup>1</sup>. Because the most recent MLS samples can still be 1/13 or 1/39 seconds old, the position

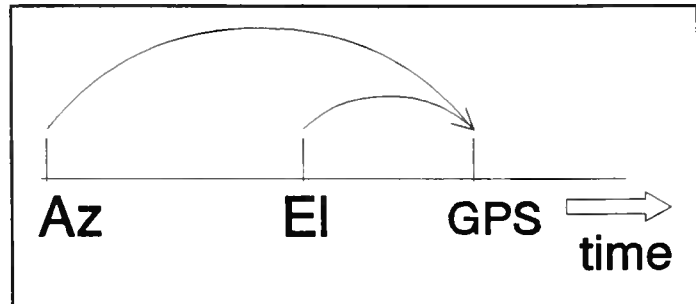


Figure 3.5 Solution 1: use new GPS and old azimuth and elevation.

calculation won't be optimal. The size of the resulting errors is calculated in appendix C. Another disadvantage is that the position information is calculated only a few times per second, depending on the update rate of the slowest information source, which may be too slow for an approach and landing.

The second solution is much more complicated. In this case, the subsystem information is processed by an estimation algorithm as soon as it arrives at the MIAS computer. The algorithm calculates an estimate of the subsystem parameters at any time. For example the GPS pseudo ranges of previous measurements are used to calculate an estimate of the pseudo ranges a little time ahead. This is in fact prediction. If this is done for the GPS ranges<sup>2</sup>, the MLS elevation and azimuth, the DME/P distance and the attitude angles, all subsystem parameters can be estimated to one common instant. This is shown in figure 3.6 for MLS, GPS and attitude.

<sup>1</sup> Assuming a GPS sampling rate of 1 sample per second.

<sup>2</sup> The GPS satellite positions are calculated as function of time. They don't have to be predicted. The MLS transmitter positions don't change as function of time, so they don't have to be predicted either.

This algorithm has the advantage of using all information available. Further, the position can be calculated as often as needed. Note that by predicting the subsystem parameters a little further ahead, the position can be calculated at a time that has still to come. This allows the calculation delay to be compensated. The error of the position can be smaller, but it largely depends on the errors made by the estimators, because the errors made by the estimators will cause errors in the position calculation.

The estimators used in this proposition can be for example Kalman estimators. [19] describes how Kalman algorithms can be used to process asynchronous samples.

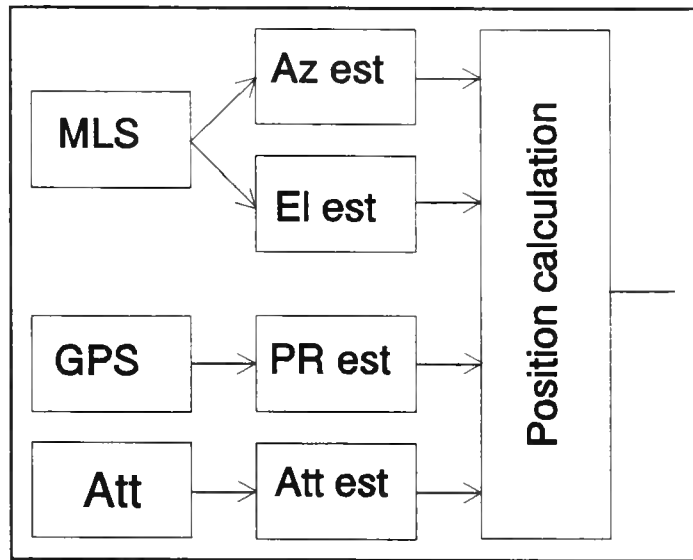


Figure 3.6 Solution 2: Use estimators and calculate the position with the estimated parameters.

### 3.5 Integrity

Integrity is the property of a system to provide timely warning when the system accuracy deteriorates beyond a certain value. It is therefore necessary to define an accuracy threshold beyond which an alarm should be given to the user of the system. Also a maximum delay between the occurrence of the accuracy threshold cross over and the alarm should be defined.

For MIAS the accuracy threshold will be derived from the ILS Cat. III accuracy, at the runway threshold. The accuracy threshold at other points in space is dependent on the MLS, DGPS and DME/P attainable accuracy. The maximum delay between the crossing of the accuracy threshold and the alarm is derived from the MLS specs and is one second.

There are several ways to implement the integrity monitoring function: the ground equipment provides warnings or the airborne equipment provides warnings. Using the airborne equipment has the advantage that the integrity of the system can be assured independent of the ground equipment. Using the ground equipment to assure the integrity also requires major modification of the existing systems. Because the MLS signals are monitored on the ground, a failure in the MLS signals can be detected and the airborne MLS receiver can be warned. This warning is used by MIAS to monitor the MLS measurements. Besides this MLS integrity check, MIAS uses a Receiver Autonomous Integrity Monitoring (RAIM) algorithm to monitor the accuracy of all measurements.

The RAIM algorithm uses two stages: detection and identification. If the erroneous measurement can be identified, the proper positioning result can be displayed and no alarm needs to be raised. The erroneous source, could still be used for positioning, because the error caused by that source might be temporary. As long as the source does not work properly, the identification will cause the faulty measurement to be identified. This statement only holds if there are enough measurements available. If one source is identified as being bad, and the number of measurements drops below the number of measurements needed for identification and an error is detected, the previously identified bad source should be excluded. In that case, no identification can be made, but knowledge about a previously identified bad source can be used. If the number of measurements drops even further, the previously identified bad measurement source should be excluded always.

Detailed information about integrity can be found in [8]. The next section describes the detection followed by the identification.

### 3.5.1 Detection

If the number of unknowns of the position estimate is 'n' and the number of measurements is 'n+1', then it is possible to calculate 'n+1' positions using 'n+1' different subsets of 'n' measurements for each position. For example: if MIAS measures elevation, azimuth and three GPS pseudo ranges, five measurements are available and four unknowns need to be calculated. Then five positions can be calculated using five different subsets of four measurements. If the measurements are numbered from A to E, the possible combinations are as follows: (A,B,C,D), (A,B,C,E), (A,B,E,D), (A,E,C,D) and (E,B,C,D). If the accuracy of none of the

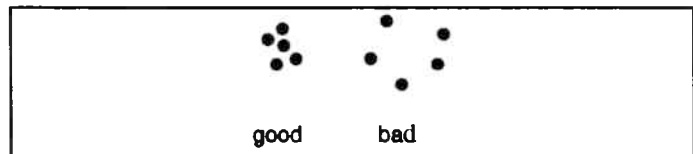


Figure 3.7 Two situations with five positions: one with sufficient accuracy and one with insufficient accuracy.

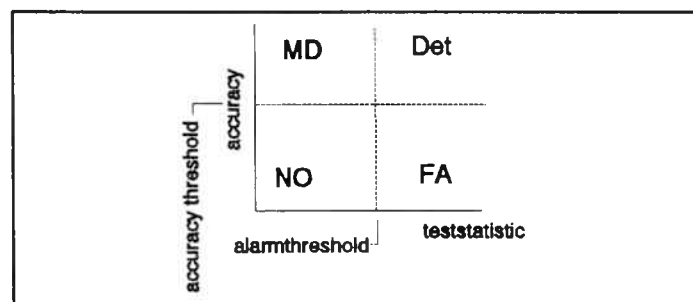


Figure 3.8 The test statistic gives the relation between the a accuracy and the measurements.

measurements is beyond the accuracy threshold, the five calculated positions will be near each other. If the accuracy of one or more of the measurements passed the accuracy limit, the positions will be further apart, see figure 3.7. The sum of the distances between the calculated positions is a measure for the accuracy of the position estimate. If the sum exceeds a certain threshold, an alarm is raised. The

sum is an example of a test statistic and the threshold is an alarm limit. This can be summarised in figure 3.8.

Figure 3.8 shows a graph with two axis: one depicts the real accuracy and the other the test statistic. In the example the test statistic is the sum of the distances between the positions of the subsets. If the test statistic crosses the alarm limit, an alarm is raised. If an alarm is raised while the real accuracy had not crossed the accuracy limit, the alarm is typified as a False Alarm (FA). These alarms are not dangerous, but should not occur too much, because the pilot might get annoyed with the alarms and might therefore ignore valid alarms. An alarm should be given when the real accuracy passes the accuracy limit and the test statistic passes the alarm limit too. This occasion is called 'Detection' (Det). This is a safe situation, because the system has warned the pilot that it is not operating well. If the accuracy passed the accuracy limit and the test statistic did not pass the alarm limit, a dangerous situation occurs called 'Missed Detection' (MD). In that case the system is not operating well, but no alarm is raised. The probability of a MD should not exceed one time in  $10^9$  flying hours or once per  $10^9$  approaches. This number is derived in [12]. The last situation is the Normal Operation (NO), where the real accuracy is good enough and the test statistic does not raise an alarm. The value of the accuracy limit and the alarm limit determine the probabilities of NO, FA, Det and MD. Detailed information about this can be found in [8].

The time to generate the alarm in case of an accuracy failure is mainly dependent on the time needed to calculate the different positions from the subsets. Using a fast computer, this time is well within one second.

So with five measurements (GPS, MLS, DME etc), five different 3-D positions can be calculated. The sum of the distances between the calculated positions can be used to detect an accuracy failure and raise an alarm within a second.

### 3.5.2 Identification

With 'n' unknowns and 'n+1' measurements, malfunctions can only be detected. If 'n+2' measurements are available, the source which caused the malfunction, can be identified, assuming only one source caused the malfunction. If more sources are erroneous, more measurements are needed to identify these erroneous sources.

When 'n+2' measurements are available, these measurements can be grouped in 'n+2' different groups of 'n+1' measurements. Every group but one will contain the erroneous measurement. If the detection algorithm from section 3.5.1 is executed on these groups, an alarm will be raised on all groups except one. This one does not contain the erroneous measurement. Because it is known which measurement is not included in that group, the bad source is identified. For example: there are six measurements A to F and four unknowns. The measurements can be divided in six groups containing

five measurements: (A,B,C,D,F), (A,B,C,D,E), (A,B,C,E,F), (A,B,E,D,F), (A,E,C,D,F) and (E,B,C,D,F).

Suppose the measurement from source A is erroneous. All groups contain A except the last group.

Using the detection algorithm will cause alarms on all groups except the last. In this way source A is identified as the erroneous source. If more than one source is bad, all subgroups will raise an alarm and no identification can be done with these groups.

So with six measurements, MIAS can identify a erroneous source, assuming that only one source is bad.

## 4 Operational Use

In this section the advantages and disadvantages of MIAS are discussed, followed by some suggestions for the use of MIAS in Air Transport and General Aviation and possible expansions for MIAS.

### *4.1 Advantages and limitations*

The main advantage of MIAS is its ability to identify erroneous measurements. This property allows the use of GPS during approach and landing. If for example one of the GPS measurements gets worse than a predefined threshold, the integrity routine of MIAS will identify that GPS measurement as being bad and MIAS will continue to calculate the aircraft position using MLS and DME/P, when available, excluding the bad GPS measurement. If not enough accurate positioning sources are available, MIAS will warn the pilot and he will decide to perform a missed approach.

Because MIAS is a hybrid positioning system, it is easily expandable. Other relevant positioning sensors can then be used to increase the integrity and possibly the accuracy of MIAS. Being a hybrid positioning system, MIAS allows also a graceful degradation of the positioning service. If for example the number of tracked GPS satellites is less than normal, the position can still be calculated, however the integrity gets worse. This property also allows approaches at runways where no DME/P ground station is located, because the DGPS measurements then provide the accuracy along the runway centre line. The integrity, however, is worse compared to the situation where the DME/P is used also. The same argument holds for aircrafts without a DME/P interrogator. They can approach any runway with an azimuth, elevation and data transmitter. This opens possibilities for General Aviation to use MLS for curved approach without the need of having a DME/P.

Of course MIAS has its limitations, but they are not severe. One of the limitations is the fact that the MLS ADW's are only transmitted in the MLS coverage, therefore the DGPS messages cannot be received all around the airport. This could be solved by installing omni-directional antenna's for the data transmitter. Using the OCI antenna's for data transmission is also possible, but this will probably give problems caused by interference in the regions where the radio signals of adjacent OCI antenna's are equally strong.

### *4.2 Suggestions for the operational use of MIAS*

As soon as MIAS is tested and found good enough, the question arises how to use MIAS. This section describes some ideas about how MIAS can be used in General Aviation (GA) and Air Transport (AT).

## 4.2.1 MIAS in General Aviation

As soon as the ILS service is stopped, many GA aircrafts will need an alternative. The basic MLS with the DME/P is expensive. MIAS offers an affordable alternative by combining the MLS angle and data information with the GPS range information using the MLS ADW data channel to transmit DGPS messages. Using a DME/N that may be installed already will improve the integrity of the system.

More and more GA aircrafts have a GPS receiver. By simply adding a MLS angle and data receiver and a computer, the aircraft can be equipped for precision approach and landing with a high integrity.

The smallest version of MIAS will need the pilot to select the MLS channel number. The position of the aircraft is then displayed relative to the runway on a simple display. In this simple version, no way points can be used, so only straight-in approaches are possible. The block diagram of this simple system is shown in figure 4.1.

In a more advanced version of MIAS the pilot still needs to select the MLS channel number. However, the Navigation (NAV) computer, which is added, can use way points to make a curved approach possible. The pilot can insert way points, but this only increases the pilot work load. The pilot better can select an approach name. The approach name is linked with a number of way points which are up linked by the MLS ADW channel. A proposition for up linking approaches by ATC via the MLS ADW channel is described in [13]. Therefore, the MLS ADW's are also read by the NAV computer. The NAV computer compares the actual position as calculated with MIAS, with the desired position calculated from the way points. The result is a steering command, which is displayed on a screen. This screen will display the way points and the position of the aircraft relative to the runway. It is also possible to display a tunnel in the sky, through which the pilot has to steer his aircraft. An example of the advanced version of MIAS is shown in figure 4.2.

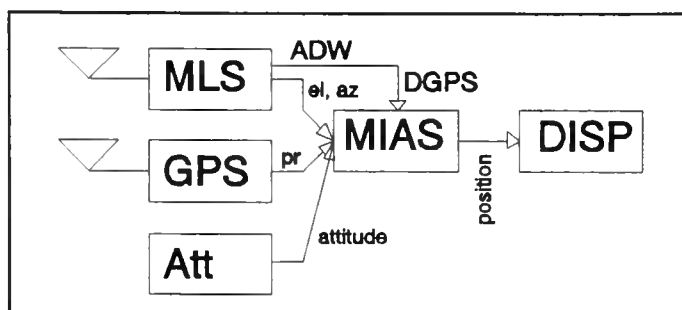


Figure 4.1 The simplest way of using MIAS.

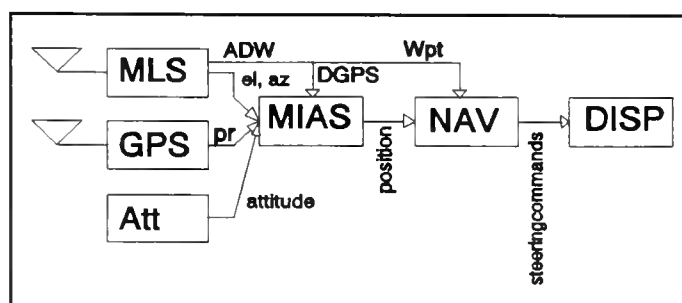


Figure 4.2 Example of advanced use of MIAS in GA aircraft.

## 4.2.2 MIAS in Air Transport

The situation in Air Transport (AT) aircrafts is different from GA aircrafts, because AT aircrafts usually have several positioning systems which are connected to a Flight Management Computer (FMC). The NAV part of the FMC calculates the position using the best set of positioning devices available.

In AT aircrafts, MIAS can replace the positioning function in the approach and landing phase of the FMC.

The navigation function cannot be performed by MIAS, so it should still be performed by the FMC. MIAS calculates the position of the aircraft using MLS, DGPS and DME/P and provides increased integrity compared to the basic MLS and DME/P. The radar altimeter, which resides in many AT aircrafts, can be used also as input for the MIAS position calculations.

Like the advanced GA version of MIAS use, the AT can also use the up linked approaches and associated way points. Although this is not necessary, because most approaches and way points are stored in the FMC back ground memory. A picture of this AT system is shown in figure 4.3.

## 4.3 Possible expansions

If the MLS data transmitter would have 360° coverage, then it would be possible to receive ADW's all around the airport. This would make it possible to determine the aircraft position with a DGPS accuracy in a busy part of the airspace. The only adjustment which would have to be made is the replacement of the MLS data transmitter antenna and the increase of transmission power by a factor 4.5<sup>1</sup>.

Although MIAS was meant to be used only in the approach and landing phases of the flight, the graceful degradation properties of MIAS make it possible to use the integrated navigation equipment for MIAS in the en-route phase of the flight as well. The navigation equipment then calculates the position using only GPS. If beside MLS other positioning devices are attached, these devices are also used to calculate the position. For precision guidance during take off, a back azimuth transmitter is

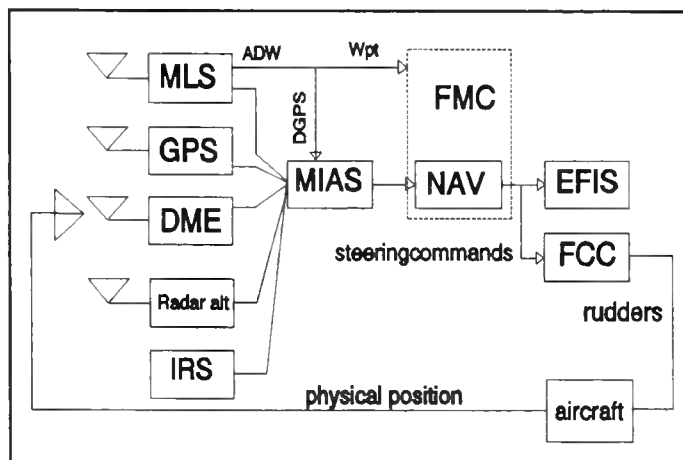


Figure 4.3 The use of MIAS in a large aircraft.

<sup>1</sup> The power is first transmitted in a V with a total angle of minimal 80°. If a 360° coverage is needed with the same power density, the transmission power should be multiplied with  $360/80 = 4.5$ .

needed. During taxiing, the MLS ADW's can probably still be received, which enables positioning with a DGPS accuracy. This may not be good enough in heavy fog, but it is still better than nothing. However reflection and shading from hangars on airports can still ruin the GPS measurements.

Loran-C can be used in some parts of Europe. Instead of transmitting DGPS messages via the MLS ADW channel, D-Loran-C messages are transmitted using the same MLS ADW channel.

# **Part II: Testing by Delft University of Technology**

## **1 Introduction**

Part II of this report discusses the effort to build a MIAS experimental airborne system and the tests which have been prepared. The airborne experiments will be performed at Schiphol Airport in Amsterdam in close co-operation with the Dutch civil aviation authority: the Rijks Luchtvaart Dienst (RLD), the faculty of Aerospace Engineering and the Dutch surveying department: the Meetkundige Dienst (MD). The MLS equipment installed at Schiphol Airport consists of a MLS azimuth, MLS elevation and MLS data transmitter and monitors. The truth reference for the MIAS airborne experiments is the position as calculated from the differentially corrected GPS integrated carrier phase measurements.

During the airborne experiments data is collected to experiments with the MIAS algorithm. During these experiments the lowest DGPS update rate possible will be determined, without compromising on accuracy while maintaining a high integrity. Further simulations are necessary to gain knowledge about handling asynchronous samples.

The aim of the testing of MIAS by Delft University of Technology (DUT) is to verify if MIAS can provide guidance during the approach and landing with an accuracy equal to MLS and a higher integrity and a small load on the MLS ADW channel.

In the following sections, the hard- and software for the MIAS experiments is described, followed by a description of how simulations, static and dynamic tests can be performed.

## 2 Hardware and software

This section describes the hardware and software for the experimental implementation of MIAS.

### 2.1 MIAS hardware

The MIAS experimental hardware is shown in figure 2.1. This section describes all the pieces of hardware used in the experimental MIAS system, starting with the most essential hardware: the aircraft. After that a description of the MLS and GPS receiver and the attitude sensor is given.

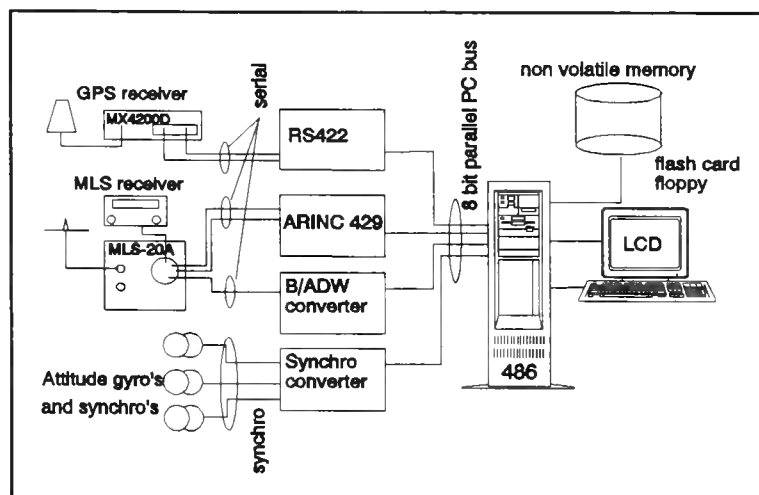


Figure 2.1 The experimental airborne part of MIAS.

#### 2.1.1 The test aircraft: the DHC Beaver

The aircraft used for the MIAS flight tests is a DHC Beaver<sup>1</sup>. The Beaver is a single engine, high wing, tail wheel aircraft and allows four to six persons to be transported. Figure 2.2 shows a sketch of the aircraft. It also shows the approximate location of the MLS and GPS antenna's. The GPS antenna is of course on top of the aircraft, because it needs to receive signals from satellites above. The GPS antenna is a patch antenna with built in preamplifier from Sensor Systems Inc.

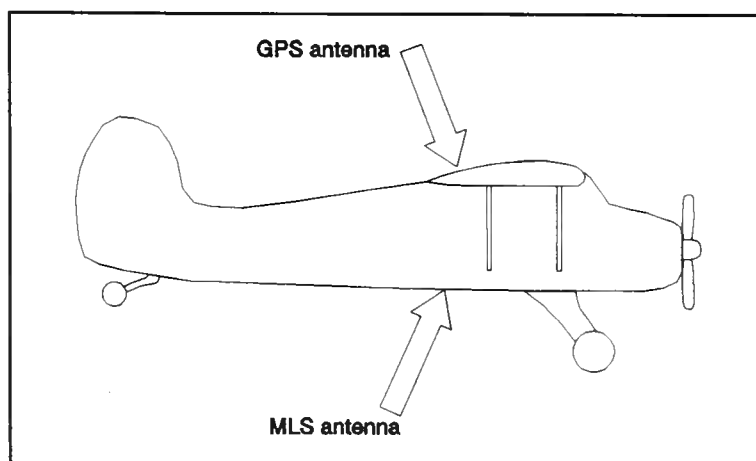


Figure 2.2 Antenna's on the Beaver

<sup>1</sup> The Beaver is owned by the faculty of Aerospace Engineering of this university. The faculty of Aerospace Engineering has been very helpful with equipment, manpower and knowledge to help the MIAS project.

The MLS antenna is at the bottom of the aircraft, aft of the main landing gear, because mounting the antenna on top of the aircraft would cause shadowing problems. This problem is caused by the high pitch angle of about  $6^\circ$  when landing at a  $3^\circ$  glideslope. The MLS antenna used is a simple dipole on a ground plane.

The position of the antenna's on the aircraft should be measured to be able to adjust the measurements as described in section 2.4. The reference system for these measurements should be an aircraft fixed reference system, because the measurements have to relate two positions within the aircraft with each other. The origin of the reference system is arbitrary, since not the position, but the vector between two positions is used. The directions of the axis of the reference system should however be parallel to the along axis, the across axis and the top axis, because these are the axis around which the roll, pitch and heading are measured.

The position of the landing gear or the CG can be calculated during the flight tests, but only the position of the GPS antenna can be checked with the truth reference system. The truth reference uses the GPS integrated phase measurements, so the position of the GPS antenna can be determined with a high accuracy during post processing.

### 2.1.2 The MLS receiver: Bendix MLS 20-A

For the MIAS experiments, a Bendix MLS 20-A receiver set<sup>1</sup> is used. This set consists of an angle and data receiver unit and a Control Display Unit (CDU). During the MIAS experiments, the CDU is only used to select the MLS channel. The MLS receiver outputs information in three ways: as an ARINC 429 data stream, as a demodulated DPSK stream and as currents for a Course Deviation Indicator (CDI).

The ARINC 429 data stream outputs azimuth, back azimuth and elevation angle information at a rate of 100 Kbit per second. Per angle measurement it also indicates which antenna is used (for or aft) and what the operating mode of the receiver is (test or normal). The angle measurements are not filtered. This ARINC 429 output is connected to a ARINC 429 card, which interfaces the MLS receiver and the MIAS computer. More information about ARINC 429 and the ARINC 429 interface card can be found in [5], [15], [16] and in appendix F and G.

The demodulated DPSK stream comes directly from the Differential Phase Shift Keying (DPSK) demodulator. The bits come out serially as a bipolar asynchronous return to zero signal with peak voltages of +5 and -5 Volts at a rate of 15625 bits per second. This is the MLS DPSK data rate. The DPSK data contains the MLS preambles and data words. Only the DPSK data contain MLS BDW's and ADW's, because the MLS receiver does not output them via the ARINC 429 output. Via

---

<sup>1</sup> The Bendix MLS 20-A with antenna is loaned to us by Ohio University (OU) in the U.S. OU has been very helpful in providing equipment and knowledge about MLS.

the DPSK output, also the bit error rate of the MLS ADW channel can be investigated. The DPSK output is connected to a BDW/ADW card, which shifts the serial bits into a register and interrupts the MIAS computer as soon as a preprogrammed bit pattern is recognised<sup>1</sup>. Then the bits can be read by the MIAS computer in parallel.

The MLS receiver can also drive a CDI, which displays the measured angles using needles. The needles are driven by currents. By connecting an ammeter to each of the outputs (one for azimuth and one for elevation), the angle measurements can be monitored. Current outputs are also used to drive flags on a CDI. These flags can also be monitored using an ammeter.

### 2.1.3 The GPS receiver: Magnavox MX4200D

For the MIAS experiments, a Magnavox MX4200D receiver is used. The MX4200D is a L1 frequency receiver which provides Standard Positioning Service (SPS). This six channel receiver has four outputs and two inputs. All in- and outputs are Electronic Industries Association (EIA) RS422 compatible. The RS422 characteristics can be summarised as a serial, asynchronous, balanced bit stream using stop bits to end a package of bits and parity bits to protect the package, see [23, p.77]. Two in- and outputs are connected to a RS422 card, which interfaces the GPS receiver and the MIAS computer, but only one input and two output channels are used.

The used input is the control input and is used to program some parameter which influence the operation of the GPS receiver. For example the elevation mask angle and the horizontal acceleration factor can be programmed. Also time recovery mode can be selected by programming. This mode will synchronise the receiver clock to the GPS time. This means that the receiver clock will indicate the GPS time. The greater the horizontal acceleration factor, the greater the bandwidth of the positioning filter and the greater the noise influence on the measurements.

One of the used output ports sends navigation and status data in a National Maritime Electronics Association (NMEA)-183 format, see [20]. These data contain the position as calculated by the receiver and status messages about the geometric strength of the position solution. This channel is used to monitor the number of satellites being tracked.

The other output, which is used, is called the raw data port. It sends messages containing the pseudo range, integrated carrier phase measurements, code offset and the GPS data as sent by the satellites. This information is used to calculate and correct the pseudo range and to calculate the satellite positions.

The integrated carrier phase of the raw data output is also used as input for the truth reference during the flight tests. The ambiguity of the integrated carrier phase is solved during post

---

<sup>1</sup> If the bit pattern is damaged due to an error in transmission, no interrupt is given and the bits are lost. This way of monitoring the bit error rate is therefore not correct. For the bit error rate, all bits should be monitored, one by one.

processing<sup>1</sup>. This method is sensitive to cycle slips due to large accelerations. When sufficient satellites are tracked, these cycle slips can be fixed. The accuracy of this positioning method is about 20 cm.

More information about the Magnavox MX4200D GPS receiver can be found in [20] or in appendix E.

## 2.1.4 The IRS

The Beaver does not have a real IRS, instead it uses two gyro's. Each points to a different direction. Both gyro's have two degrees of freedom. One gyro points to the local vertical and is kept pointing there by the earth's gravitation. The angles between this gyro and the aircraft frame are the roll and pitch angles. The second gyro points North. It is kept pointing North by a flux valve, which measures the earth's magnetic field. This causes the gyro to point to the magnetic North instead of pointing to true North. So by measuring the angle between the gyro and the aircraft frame, the heading can be determined<sup>2</sup>. A gyro slaved by a flux valve is called a gyrosyn. More information about gyro's and flux valves is in [1].

Because the WGS-84 reference system uses meridians which run from true South to true North, the heading angle should be the angle between the true North direction and the aircraft along axis. The magnetic North heading can be adjusted to True North using an offset. This offset is dependent on the position on earth.

The angles of the gyro's with the aircraft frame are measured using so called AC synchro's. These devices amplitude modulate the measured angle on a 400 Hz carrier using three wires and two reference wires. These synchro's measure roll, pitch and heading. The synchro signals are connected to a synchro to digital converter, which interfaces the MIAS computer and the synchro's. More information about synchro's and the synchro to digital converter is in [22] and appendix G.

Because of mounting inaccuracies, the synchro's introduce an offset in the roll, pitch and heading measurements. Because the antenna positions were measured using the aircraft reference system, the roll, pitch and heading should be without offset. If the angles have an offset, these offsets would make the position calculations worthless. If the aircraft is parked, the roll offset can be measured easily. The aircraft wings are level with the ground and the size of the roll offset is the angle indicated by the roll synchro to digital converter. The pitch offset can be measured after the tail of the aircraft is jacked up until the artificial horizon indicates a zero pitch angle. The size of the pitch offset

---

<sup>1</sup> The Surveying department (MD) of the Dutch Government has been found willing to process the integrated carrier phase measurements to find the position of the GPS antenna. They also surveyed the location for the DGPS reference station.

<sup>2</sup> The second degree of freedom of this gyro is used to keep the gyro level.

is then the angle indicated by the pitch synchro to digital converter. The size of the heading offset is the difference between the gyrosyn compass reading and the angle indicated by the heading synchro to digital converter.

### 2.1.5 The MIAS computer: IBM compatible 486 PC

The devices mentioned in the previous sections are connected to the MIAS computer, which is a IBM compatible PC with a 80486 33 MHz processor. The PC board is mounted in a desktop frame and has eight extension slots. The extension cards used are: an ARINC 429 interface, a RS422 interface, a three channel synchro to digital converter, a BDW/ADW converter, a flash memory card, an I/O controller and a video board.

The hard disc won't be used during the flight tests, because of its sensitivity to vibrations. Instead, a flash memory card is used. This card contains 12 Mb of Electrically Erasable Programmable Read Only Memory (EEPROM), which hold its information even if the power is shut off.

The video card is used to drive a Philips monochrome LCD screen<sup>1</sup>. The video screen is only used to check if all devices work properly and to execute DOS commands if necessary.

### 2.2 MIAS software philosophy and hierarchy

For the MIAS experimental airborne system, software was written. A stripped version of this software will be used in the flight testing, because it only has to collect information during the flight. The information is then stored on the flash memory card with a time tag to be able to process the data later in the full software. The time used for the time tag is the PC clock time. This time has an offset with respect to the GPS time, but this offset can be solved easily using at least four positioning sources. The software was built with a certain philosophy, which will be described now.

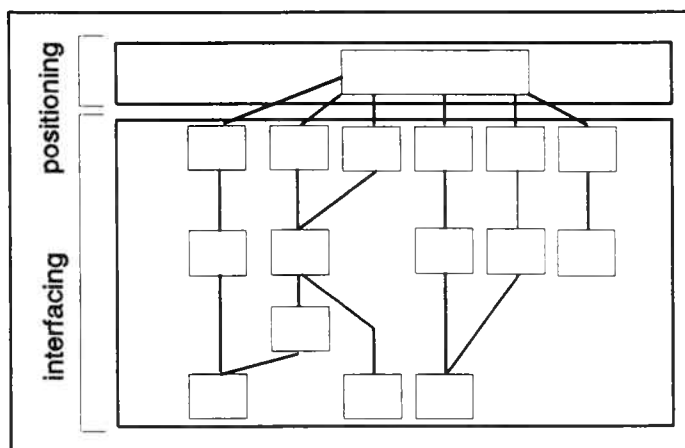


Figure 2.3 Interfacing and positioning software

<sup>1</sup> This LCD screen could be borrowed from the faculty of Physics of Delft University of Technology (DUT).

A top down approach of the programming problem made the experimental MIAS software easily expandable. The software has therefore become very structured. The fact that not all sensors were available at the same time stimulated this particular structure.

The software can be divided in two parts. First there is the interface section. This section is the connection between the computer communication facilities, and the positioning software. The second part contains the positioning software. Figure 2.3 illustrates the division between interface and positioning software.

Besides this division, there is a second division possible. The first part of it is dependent on the type of sensors used. Different brands or types of sensors need different pieces of software. The second part is hardware independent. It doesn't have to be changed when using other hardware, i.e. different pieces of hardware with the same function e.g. a GPS receiver. In figure 2.4, the division between hardware dependent and hardware independent software is shown.

There is at least one more way to look at the written software. The software can be seen as the implementation of a quasi OSI model<sup>1</sup>. This is shown in figure 2.5. Starting at the top of the picture and descending, the functions get more specific and more fundamental. At the bottom of the picture, only standard

procedures, functions and statements are used. Level 0 is the electrical level where currents and voltages are generated and measured. Level 1 is the driver level. In this level routines instruct the interface chips to perform their tasks and deliver bytes or bits. Level 2 is an adjustment of level 1 to level 3. Level 3 contains routines which collect the bytes from level 1 and 2 and forms messages from

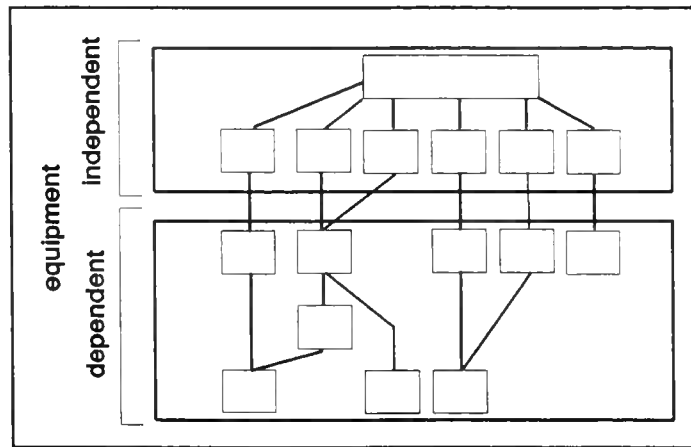


Figure 2.4 Hardware dependent and hardware independent parts of the software.

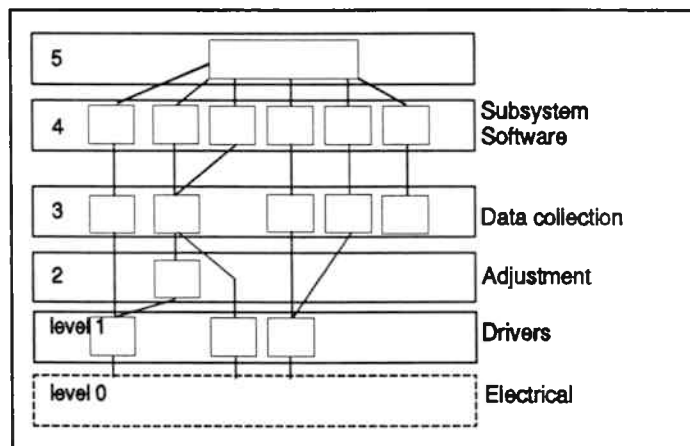


Figure 2.5 MIAS software as OSI system

<sup>1</sup> Open Systems Interconnection, [23].

them, which are converted to variables. Level 4 uses the variables to perform the subsystem specific calculations. Level 5 calculates the position.

The MIAS experimental software is described in detail in [17].

### 3 Test setup

This section describes the different ways of testing MIAS. First simulations are considered, followed by static tests. The flight tests and post processing conclude this section.

#### 3.1 *Simulation of MIAS*

Simulating MIAS has the advantage, that all flight condition and all transmitter conditions can be investigated and can be repeated over and over. Besides, simulation is very cheap, compared to real flying.

For simulating MIAS, a choice can be made whether to simulate only the GPS, DME and MLS transmitters or both the GPS, DME and MLS receivers and transmitters. To simulate the attitude information the IRS needs to be modelled. A third possibility is using simulation software, which simulates the entire MIAS system.

If only the GPS, DME and MLS transmitters are simulated, simulators are used to generate radio waves, which are fed to the GPS, DME and MLS receiver. This simulation requires special costly GPS, DME and MLS simulators, but the complete MIAS airborne part can be simulated. The simulators need a model of the GPS and MLS transmitters and the propagation of radio waves. The model will determine the accuracy of the simulation.

The second possibility is much cheaper and does not require special devices. Instead of attaching a MLS, DME and GPS receiver to the MIAS computer, another computer is attached. This computer then sends GPS, DME and MLS receiver messages to the MIAS computer. The messages are calculated for the flight trajectory of a virtual aircraft. The simulator needs a good model of the GPS, DME and MLS transmitters and receivers and the propagation of radio waves. This model will determine the accuracy of the simulation.

A third possibility, which is even cheaper, uses a special program which contains routines for simulating the MLS, DME and GPS transmitters and receivers, the propagation of radio waves and MIAS. The accuracy of this simulation again depends on the model of the GPS and MLS transmitters and receivers, the propagation of radio waves and the model of the MIAS algorithm.

### 3.2 MIAS static testing at Schiphol Airport

For static tests of MIAS, it is necessary to be in the MLS coverage to be able to receive MLS signals. The nearest airport with a MLS installation is Schiphol Airport<sup>1</sup> (Amsterdam). Because the MLS coverage in the approach region inclines with an angle of  $0.9^\circ$  from the MLS datum point, it is necessary to find a high enough building in the vicinity of the runway. This is shown in figure 3.1.

The data collection version of the MIAS software was tested on the roof of a building<sup>2</sup> just within the MLS coverage. Figure 3.2 shows the location of the building relative to the runway. The data collection was tested at Schiphol to be sure that the data collection would work fine when flying.

The results of the test were that the data collection worked properly.

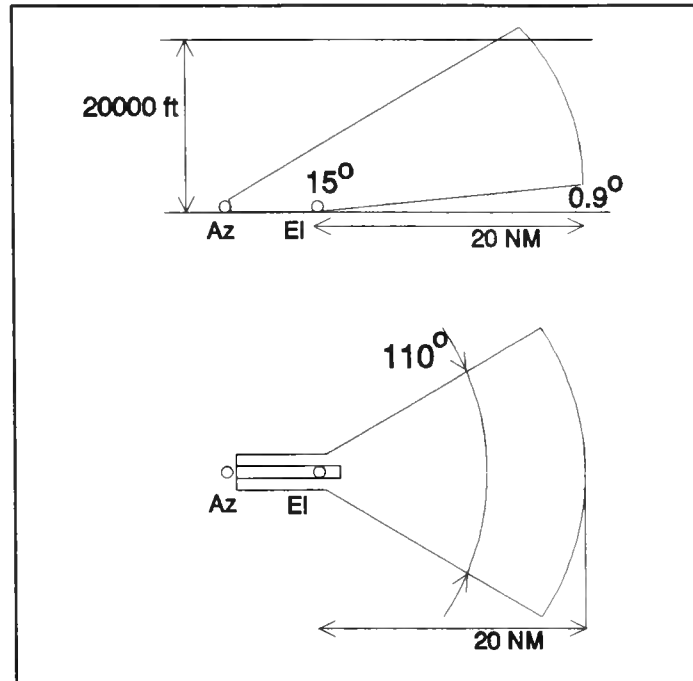


Figure 3.1 The MLS coverage around the runway at Schiphol.

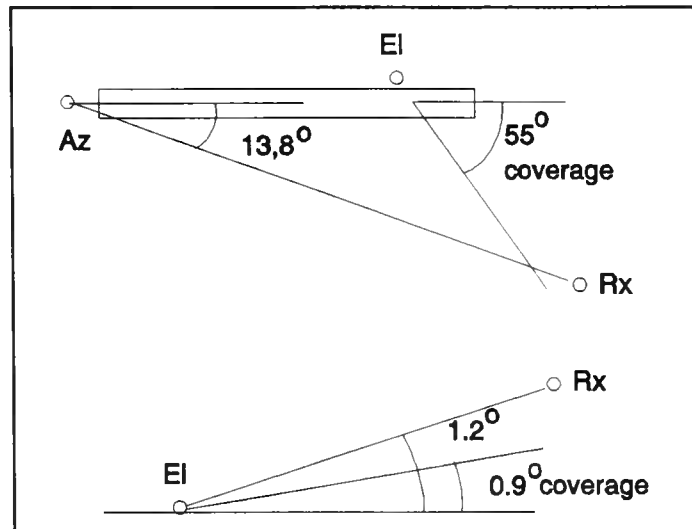


Figure 3.2 The runway, MLS transmitters and measuring site, showing the azimuth and elevation angles at Schiphol.

<sup>1</sup> The MLS installation is located at runway 01R and the channel number is 548.

<sup>2</sup> The Yamaha company was so kind to allow measurements to be taken on the roof of one of their buildings under construction.

### *3.3 Flight data collection with the DHC Beaver aircraft*

To verify the MIAS concept, flight data is necessary. Therefore flight tests are planned at Schiphol Airport in March 1993 to collect MLS, GPS and attitude data. GPS data will be collected at the same time on a surveyed spot near the runway to be used for DGPS message calculation. The collected data will be processed after the flight tests have finished. Using the GPS data of the surveyed point, different DGPS update rates can be simulated giving different ADW channel loads during post processing.

The truth reference for the flight tests will be calculated from the GPS integrated carrier measurements. By solving the cycle ambiguity, the position of the GPS antenna can be calculated. This position will be used as a reference for the MIAS calculations.

The flight tests have not yet been performed.

### *3.4 Suggestions for post-flight processing*

The collected MLS, GPS and attitude data from MIAS flight tests do not say anything about the performance of MIAS by themselves. Therefore the data has to be processed by the MIAS algorithm. Because the program written for the experimental MIAS airborne part is not fit to process the data, a new program has to be written. This section lists some suggestions on the structure to be used to process the flight data.

#### 3.4.1 Structure of the post flight test program

During the flight tests, the data from MLS, GPS and the attitude is collected and stored using a time tag. The time tag indicates the reception time at the GPS receiver. The GPS receiver on the surveyed site does the same. Because of the time tag, the information from the subsystems can be split, without losing the order in which the information was read. Splitting the information makes the programming of the post flight test program a lot easier and clear.

The stored information comes in two files: one for the flight data and one for the DGPS reference station data. The flight data is split into: GPS ephemeris, GPS pseudo range information, MLS azimuth, MLS elevation, MLS data, roll, pitch and heading. The DGPS reference station file is split in ephemeris and pseudo range information.

The truth reference is separately calculated and will need the GPS integrated carrier phase measurements and ephemeris information. Therefore another file is made containing all GPS carrier phase and ephemeris information from the flight. This file is used to calculate the position of the

aircraft. This position is used as a reference for the MIAS calculations. The reference positions are then available in a file having the GPS receiver time as time tag.

Because in the MIAS concept the DGPS reference station will work independently of the aircraft, the post flight processing of the DGPS reference data should be done independently too. This has the advantage, that the processing can be split in several stages. First the DGPS messages are calculated and stored using the time of arrival at the aircraft as time tag. Then the MIAS airborne routines can start using the DGPS messages.

The post processing can be summarised as follows: split the flight data file in: ephemeris, pseudo ranges, azimuth, elevation, roll, pitch and heading. Split the DGPS file in ephemeris and pseudo ranges. The flight data file is used to generate a truth reference file containing all GPS information. This file gives the 'real' positions of the aircraft after the ambiguities are solved. Then calculate the DGPS messages, followed by the MIAS position calculation. Finally compare the MIAS positions to the truth reference position.

### 3.4.2 The DGPS message post processing routine

The DGPS message routines will first read the ephemeris file until enough ephemeris information is available to start the DGPS message calculation. The time tag of the last ephemeris update is remembered. The routine will then start reading in the pseudo range file, and each time tag is compared with the ephemeris time tag, which was remembered. As soon as the pseudo range time tag is later than the ephemeris time tag, the pseudo range information can be used to calculate the DGPS messages. As soon as a DGPS message is calculated, it is stored in a new file with a time tag which accounts for calculation delay, transmission delays and receiver acquisition delay. The next step is to read the ephemeris file and the pseudo range file line by line until the time tags are  $x$  seconds later than the time tag of the previous DGPS message. Where ' $x$ ' is the inverse of update rate chosen for the DGPS messages. Again a DGPS message is calculated and this whole process repeats until the files end.

It may not be necessary, but it is wise to check the ephemeris information for time out. The ephemeris is valid for four to six hours.

The DGPS routine can be summarised as follows: read ephemeris until enough information is available to work with, read pseudo range until the starting point is reached, calculate DGPS message and store them with proper time, read ephemeris and pseudo ranges until the next DGPS message is necessary. This process is repeated until the file ends.

### 3.4.3 The MIAS post processing routine

The routine to process MIAS is similar to the DGPS routine. First the ephemeris file is read until two satellites can be used. Then the pseudo ranges are read until the starting point is reached, which is the time where two ephemerids became available. Then the DGPS message file is read until the starting point is reached. The DGPS messages before the starting point should be remembered with their time tag. The DGPS information can be used until a new DGPS message arrives or as long as it is valid. After a certain predefined time, the accuracy of the DGPS message is too bad to be used. The next step is to read the azimuth and the elevation files until the starting point is reached. If no elevation and azimuth was available, the GPS, DGPS and MLS files are read line by line until four or more pseudo ranges and ephemerids are available, or azimuth and elevation and two or more pseudo ranges and ephemerids. The time tag where this condition became true is remembered. Then the roll, pitch and heading file is read until the time tag just acquired. If the angles are available, the GPS measurements can be corrected using the DGPS messages and the time, after which the MIAS position can be calculated. The MIAS position is then stored in a file with a time tag and a code describing which satellites and MLS angles were used. After the calculation also an integrity routine can be run. This whole sequence is repeated until the files end.

For the airborne part of MIAS it is necessary to monitor the age of the DGPS messages. It may not be necessary, but also the age of the ephemeris message should be monitored.

The MIAS routine can be summarised as follows: read ephemeris until two satellites are available, read DGPS file, read MLS files. If enough information is available, read the attitude file. If enough information is available, calculate corrected GPS ranges and the MIAS position. Run the integrity routine and store the information in a file. Repeat the sequence until the files end.

### 3.4.4 Comparing the MIAS position to the Truth reference

From the routines described in the previous sections, two files result: one with the 'real' position of the aircraft, and one with the position as calculated with MIAS, containing also information on the satellites used and possible warnings. The positions in these files can be compared with each other to check the performance of MIAS.

One way of determining the performance of MIAS is the statistical way by calculating the average error and the standard deviation in three dimensions. Another one is graphical and shows three graphs, one for each position coordinate, as function of time. The graphs show the MIAS position and the truth reference position. The most interesting part of the flight is of course the part just before touchdown. The accuracy of this part of the flight is specified and the results of MIAS can be checked against these specification.

## Conclusions and recommendations

As it was stated in the introduction, the aim of the research for this report is to design and implement the airborne part of a MIAS experimental system and to evaluate it. In this report, the design and implementation of the MIAS airborne part is described. MIAS can use MLS, DME, GPS and IRS information. The experimental MIAS airborne system uses only MLS, GPS and IRS information.

During the design of the MIAS airborne system several problems were detected and solved. One of the problems is to extract as much information from asynchronous samples as possible to calculate the position of the aircraft with these asynchronous samples. Another problem is to minimise the load of the MIAS DGPS messages on the MLS ADW channel. A first estimate of the MIAS DGPS load on the MLS ADW channel indicates MIAS uses 9.14 or 19.27 .

To evaluate the MIAS airborne part, an experimental system was build. Although the implemented system functions properly, it still needs some modifications to extract as much information as possible from the asynchronous samples. Furthermore, the DGPS software, which has to calculate the GPS corrections as a function of time from the DGPS messages is not available yet.

The MIAS experimental airborne system as it was developed has not been tested thoroughly yet. Only the subsystems and their interface to the MIAS computer have been tested. These tests were successful; all interfaces operated correctly. The actual testing of the MIAS system will be done using static tests, at a building near Schiphol Airport. Flight tests are planned, during which the MLS, GPS and IRS information is stored. At the same time, GPS information is stored at a surveyed point, to be able to calculate DGPS messages. These data will be processed after the flight to enable variable DGPS message update rates to be evaluated. The truth reference for these flights will be the GPS integrated carrier phase measurements.

Because the MIAS airborne system is a modular system, it can be expanded quite easily. Extra positioning sensors like a DME can be added to provide higher accuracy and higher integrity.

It is recommended that:

- Estimators are used to be able to calculate sensor information in advance, based on previous measurements. This will tackle the problem of asynchronous samples better than the present solution. Kalman algorithms are currently under investigations as candidates to function as estimator.
- DGPS software is included. This software is under development.
- MIAS is tested more thorough using static and dynamic tests, but also simulations should be considered.
- For the evaluation of the MIAS test, post processing and possibly simulation software needs to be developed.
- Further research is done to find out which positioning sensors can be added to MIAS to improve the accuracy and integrity of MIAS.

## Literature

- [1] Abbink, F.A.,  
Course notes on LR93I Vliegtuiginstrumentatie I in Dutch.  
Delft: Delft University of Technology, faculty of Aerospace Engineering, Stability and Control group, July 1984.
- [2] Aeronautical Telecommunications Annex 10, Vol. 1 fourth edition.  
International Civil Aviation Organisation, April 1985.
- [3] Annex A to STANAG 4294 subj: NAVSTAR GPS system characteristics, Draft issue L.  
MAS NATO, 1 August 1990.
- [4] Almering, J.H.J.,  
Analyse, 5<sup>e</sup> druk in Dutch.  
Delft: Delftse Uitgevers Maatschappij, 1988.
- [5] Arinc specification 429-12, Mark 33 digital information transfer system (DITS).  
Annapolis, Maryland: July 1990.
- [6] Arinc specification 727, Airborne Microwave Landing System Receiver.  
Annapolis, Maryland.
- [7] Arinc specification 743, Airborne Global Positioning System Receiver.  
Annapolis, Maryland: March 1990.
- [8] Benckhuisen, H.C.F.,  
Integriteit, thesis report in Dutch.  
Delft: Delft University of Technology, Faculty of Electrical Engineering, November 1992.
- [9] Berghuis van Woortman, H.J.,  
Course notes on LR94 Cursus Luchtverkeersleiding in Dutch, issue 5.  
November 1991.
- [10] Brouwer, F.J.J.,  
GPS, navigatie en geodetische puntsbepaling met het Global Positioning System.  
Delft: Delftse Universitaire Pers, 1989.

- [11] Burcham, K.L.,  
"Planning for complementary MLS/GPS operations".  
The Federal Aviation Administration, MLS program office.
- [12] Laginja, T.,  
"Tunnel concept RNP considerations", Working paper 133  
Montreal, Canada: All Weather Operations Panel (AWOP), Working Group, Fourth Meeting,  
19-30 October 1992.
- [13] Laginja, T.,  
"MLS RNAV Database Assignment Example: Guidance Material for Annex 10", Working  
paper 142  
Montreal, Canada: All Weather Operations Panel (AWOP), Working Group, Fourth Meeting,  
18-30 October 1992.
- [14] Leeuwen, R.G.A. van.,  
The geometry aspects of the MIAS-project, thesis report.  
Delft: Delft University of Technology, Faculty of Electrical Engineering, November 1992.
- [15] LIB429P Reference Guide, version 5.5.  
Quebec, Canada: Max Technologie inc.
- [16] M429PC User's guide & commands reference, version 5.  
Quebec, Canada: Max Technologie inc.
- [17] Meijer, R.C.,  
Software for the MIAS experimental Airborne system,  
Delft: Delft University of Technology, Faculty of Electrical Engineering, 1993
- [18] MLS-20A Microwave Landing System, Maintenance manual I.B.,  
2020A Bendix General Aviation, Avionics Division.
- [19] Moelker, D.J.,  
Internal report on Kalman algorithms in Dutch.  
Delft: Delft University of Technology, Faculty of Electrical Engineering, 1993.

- [20] MX4200 GPS receiver programmer's guide,  
Torrance, California: Magnavox Electronics System Company, West Coast division.
- [21] Strang, G.,  
Linear Algebra and its applications, third edition  
San Diego: Harcourt Brace Jovanovich, Publishers, 1988
- [22] Synchro conversion handbook,  
DDC, Library of Congress Catalog Nr: 74-77038.
- [23] Tanenbaum, A.S.,  
Computer Networks, second edition.  
London: Prentice Hall International, Amsterdam: Vrije Universiteit Amsterdam, 1989.
- [24] Verhoeven, R.P.M.,  
Accuracy considerations on and mathematical aspects of MLS computed centre line approaches,  
Nationaal Lucht- en RuimtevaartLaboratorium, NLR CR 89142L.
- [25] Willemsen, D.,  
A synchro PC interface for the MLS Integrated Approach System, task report.  
Delft: Delft University of Technology, Faculty of Electrical Engineering, 1993.
- [26] Willigen, D. van,  
Course notes on L104 Radioplaatsbepaling in Dutch.  
Delft: Delft University of Technology, faculty of Electrical Engineering.
- [27] Willigen, D. van and E.P.M. Vlietstra,  
"MIAS, the Integration of MLS with GPS/Loran-C",  
ION National Technical Meeting, San Diego, California, January 27-29 1992.

## Appendix A MLS time multiplex and data words

In this appendix, the basics of the MLS time multiplex are treated. First the smallest components of the multiplex signal are described. The data-words are described later in this appendix.

### A.1 MLS time multiplex

The MLS time multiplex signal consists of signals that represent several functions. There are angle functions and data functions. For example azimuth and elevation functions are part of the angle function group. Basic and auxiliary data functions are part of the data function group. Each function is preceded by a preamble, which contents are listed in table A.1. The lengths of the functions are listed in table A.2.

Table A.1 MLS function preambles, [2].

Event	Time (milliseconds)
Carrier acquisition	0
Receiver reference time code	
I <sub>1</sub> = 1	0.832
I <sub>2</sub> = 1	0.896
I <sub>3</sub> = 1	0.960
I <sub>4</sub> = 0	1.024
I <sub>5</sub> = 1	1.088
Function identification	
I <sub>6</sub>	1.152
I <sub>7</sub>	1.216
I <sub>8</sub>	1.280
I <sub>9</sub>	1.344
I <sub>10</sub>	1.408
I <sub>11</sub>	1.472
I <sub>12</sub>	1.536
End of preamble	1.600

For every function a minimum transmission rate is required. These rates are listed in table A.3. The functions are transmitted in sequences. These sequences are repeated in a jittered way and so form a full cycle. The sequences are jittered, to prevent synchronous blocking of the MLS signal by rotors or propellers. Figure C.3 shows the sequences that are recommended by the ICAO when normal azimuth functions are used. The full cycle is shown in figure C.4.

Table A.2 MLS function lengths, [2].

Function	Length (milliseconds)
Approach Azimuth	15.900
Back azimuth and High rate approach azimuth	11.900
Approach Elevation	5.600
Flare	5.300
Basic Data	3.100
Auxiliary Data	5.900

Table A.3 Minimum transmission rates for MLS functions, [2].

Function	Average transmission rate (per second)
Approach azimuth	13 ± 0.5
High rate approach azimuth	39 ± 1.5
Back azimuth	6.5 ± 0.25
Approach elevation	39 ± 1.5
Flare elevation	39 ± 1.5
Basic data-word 1, 3, 4, 5, 6	1
Basic data-word 2	6.25
Auxiliary data-word A1, A2, A3, A4	1

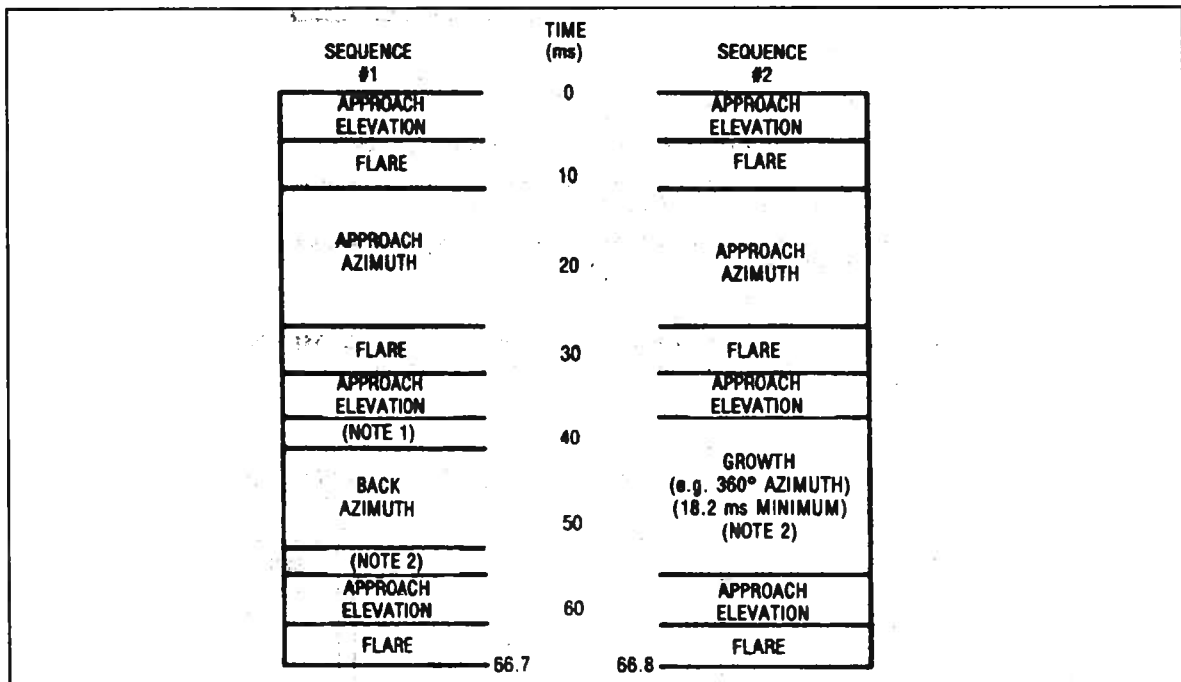


Figure A.1 Recommended sequences, [2].

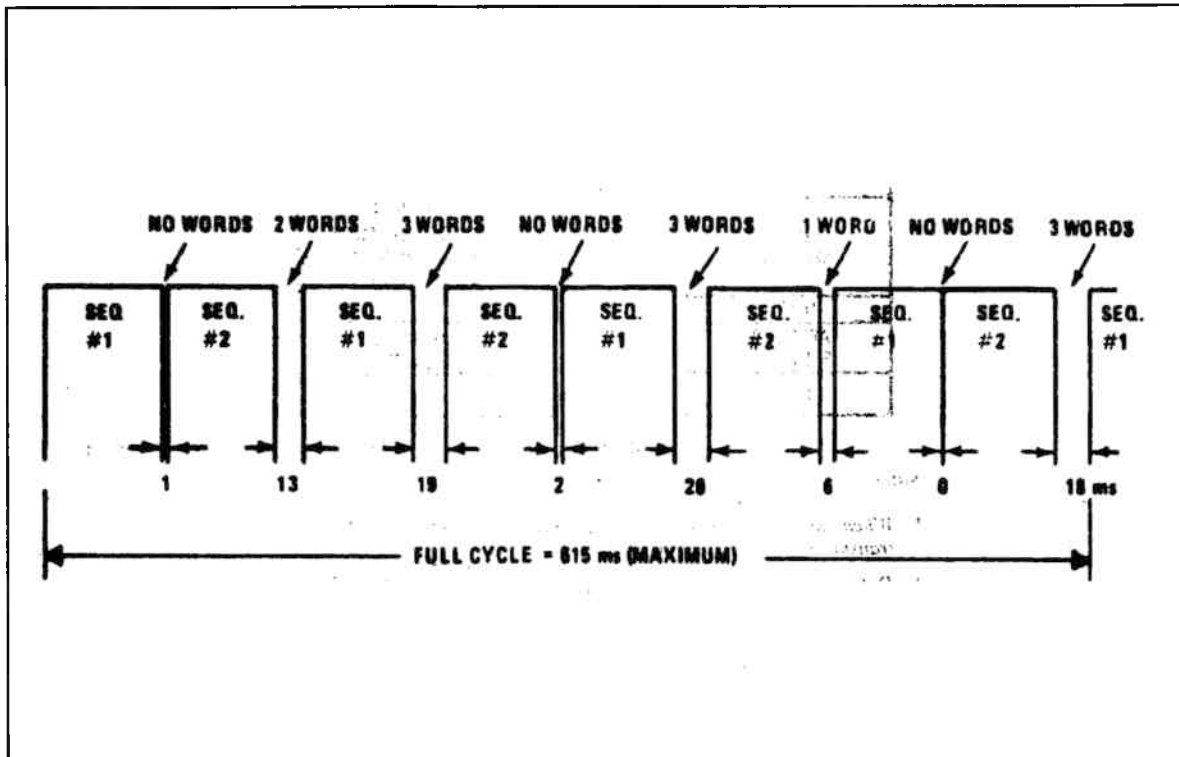


Figure A.2 Recommended full cycle for MLS functions, [2].

In the MLS multiplex scheme, the azimuth transmitter is the master and the elevation and other transmitters are slaves. This means that the azimuth transmitter decides which transmitter may transmit. The azimuth transmitter then signals the appropriate transmitter to transmit. Only the azimuth equipment transmits the data words.

### A.2 MLS data words

The MLS definition by the ICAO specifies two kinds of data words: the Basic data words (BDW) and the Auxiliary data words (ADW). The BDW's are used to inform the user of certain necessary parameters concerning the MLS ground equipment. The BDW contents are listed in table A.4.

The ADW's are used for extra information concerning the MLS ground equipment or waypoint information etc. The ADW's are divided in three parts: the A, B and C words. Each of which can be subdivided in 64 different words (A1..A64 and B1..B64 and C1..C64). Currently, only ADW A1, A2, A3 and A4 are defined. The contents of these words are listed in table A.5.

If ADW's are used to transmit GPS error data, it is important to know what data rate can be expected. Therefore the cycle and sequences from figure C.3, C.4 and table A.2 are used to calculate the available slots for ADW and BDW transmission. If the flare function is not implemented (as it is now), there will be 24 flare slots and 4 growth slots available per full cycle plus 12 ADW slots between the sequences. Less than 3 BDW's and 2 ADW's are transmitted every 615 msec ( 6 BDW's and 4 ADW's per second). Every flare function can contain a BDW and 3 ADW's can be put in a growth

function. This leaves 21 flare slots, 3 1/3 growth slots and 12 ADW slots per full cycle. Because an ADW transmission is longer than a flare transmission, see table A.2, only 22 ADW's can be transmitted per full cycle or 35 per second. With 49 bits per ADW, this gives 1078 bits per full cycle or an average of about 1752 bits per second. This is the available bit rate for extra data transmission.

If the flare and growth slots cannot be used for ADW transmission, only 12 - 2 extra ADW's can be transmitted per 600 ms. This gives 16.6 ADW's per second or 817 bits per second.

Table A.4 MLS Basic Data word contents, [2].

Word	Data content	Bits	Range	LSB	bitnr
1	PREAMBLE	12			I <sub>1</sub> -I <sub>12</sub>
	approach azimuth antenna to threshold distance	6	0 to 6300m	100m	I <sub>13</sub> -I <sub>18</sub>
	approach azimuth proportional coverage negative limit	5	0 to 62°	2°	I <sub>19</sub> -I <sub>23</sub>
	approach azimuth proportional coverage positive limit	5	0 to 62°	2°	I <sub>24</sub> -I <sub>28</sub>
	clearance signal type	1			I <sub>29</sub>
	SPARE	1			I <sub>30</sub>
	PARITY	2			I <sub>31</sub> -I <sub>32</sub>
	2	PREAMBLE	12		
minimum glide path		7	2 to 14.7°	0.1°	I <sub>13</sub> -I <sub>19</sub>
back azimuth status		1			I <sub>20</sub>
DME status		2			I <sub>21</sub> -I <sub>22</sub>
approach azimuth status		1			I <sub>23</sub>
approach elevation status		1			I <sub>24</sub>
SPARE		6			I <sub>25</sub> -I <sub>30</sub>
PARITY		2			I <sub>31</sub> -I <sub>32</sub>
3	PREAMBLE	12			I <sub>1</sub> -I <sub>12</sub>
	approach azimuth beamwidth	3	0.5 to 4°	0.5°	I <sub>13</sub> -I <sub>15</sub>
	approach elevation beamwidth	3	0.5 to 2.5°	0.5°	I <sub>16</sub> -I <sub>18</sub>
	DME distance	9	0 to 6387.5 m	12.5m	I <sub>19</sub> -I <sub>27</sub>
	SPARE	3			I <sub>28</sub> -I <sub>30</sub>
	PARITY	2			I <sub>31</sub> -I <sub>32</sub>
4	PREAMBLE	12			I <sub>1</sub> -I <sub>12</sub>
	approach azimuth magnetic orientation	9	0 to 359°	1°	I <sub>13</sub> -I <sub>21</sub>
	back azimuth magnetic orientation	9	0 to 359°	1°	I <sub>22</sub> -I <sub>30</sub>
	PARITY	2			I <sub>31</sub> -I <sub>32</sub>
5	PREAMBLE	12			I <sub>1</sub> -I <sub>12</sub>
	back azimuth proportional coverage negative limit	5	0 to 42°	2°	I <sub>13</sub> -I <sub>17</sub>
	back azimuth proportional coverage positive limit	5	0 to 42°	2°	I <sub>18</sub> -I <sub>22</sub>
	back azimuth beamwidth	3	0.5 to 4°	0.5°	I <sub>19</sub> -I <sub>25</sub>
	back azimuth status	1			I <sub>26</sub>
	SPARE	4			I <sub>27</sub> -I <sub>30</sub>
	PARITY	2			I <sub>31</sub> -I <sub>32</sub>
6	PREAMBLE	12			I <sub>1</sub> -I <sub>12</sub>
	MLS ground equipment identification		A to Z		
	Character 2	6			I <sub>13</sub> -I <sub>18</sub>
	Character 3	6			I <sub>19</sub> -I <sub>24</sub>
	Character 4	6			I <sub>25</sub> -I <sub>30</sub>
	PARITY	2			I <sub>31</sub> -I <sub>32</sub>

Table A.5 MLS Auxiliary Data Word contents, [2].

Word	Data content	Bits	Range of value	LSB	Bitnr	
A1	PREAMBLE	12			I <sub>1</sub> -I <sub>12</sub>	
	address	8			I <sub>13</sub> -I <sub>20</sub>	
	approach azimuth antenna offset	10	-511 to 511m	1m	I <sub>21</sub> -I <sub>30</sub>	
	approach azimuth antenna to MLS datum point distance	13	0 to 8191m	1m	I <sub>31</sub> -I <sub>43</sub>	
	approach azimuth alignment with runway centre line	12	-20.47 to 20.47°	0.01°	I <sub>44</sub> -I <sub>55</sub>	
	approach azimuth antenna co-ordinate system	1			I <sub>56</sub>	
	SPARE	13			I <sub>57</sub> -I <sub>69</sub>	
	PARITY	2			I <sub>70</sub> -I <sub>76</sub>	
	A2	PREAMBLE	12			I <sub>1</sub> -I <sub>12</sub>
		address	8			I <sub>13</sub> -I <sub>20</sub>
approach elevation antenna offset		10	-511 to 511m	1m	I <sub>21</sub> -I <sub>30</sub>	
MLS datum point to threshold distance		10	0 to 1023m	1m	I <sub>31</sub> -I <sub>40</sub>	
approach elevation antenna height		7	-6.3 to 6.3m	0.1m	I <sub>41</sub> -I <sub>47</sub>	
SPARE		22			I <sub>48</sub> -I <sub>69</sub>	
PARITY		7			I <sub>70</sub> -I <sub>76</sub>	
A3	PREAMBLE	12			I <sub>1</sub> -I <sub>12</sub>	
	address	8			I <sub>13</sub> -I <sub>20</sub>	
	DME offset	10	-511 to 511m	1m	I <sub>21</sub> -I <sub>30</sub>	
	DME to MLS datum point distance	14	-8191 to 8191m	1m	I <sub>31</sub> -I <sub>44</sub>	
	SPARE	25			I <sub>45</sub> -I <sub>69</sub>	
	PARITY	7			I <sub>70</sub> -I <sub>76</sub>	
A4	PREAMBLE	12			I <sub>1</sub> -I <sub>12</sub>	
	address	8			I <sub>13</sub> -I <sub>20</sub>	
	back azimuth antenna offset	10	-511 to 511m	1m	I <sub>21</sub> -I <sub>30</sub>	
	back azimuth to MLS datum point distance	11	0 to 2047m	1m	I <sub>31</sub> -I <sub>41</sub>	
	back azimuth alignment with runway centre line	12	-20.47 to 20.47°	0.01°	I <sub>42</sub> -I <sub>53</sub>	
	SPARE	16			I <sub>54</sub> -I <sub>69</sub>	
	PARITY	7			I <sub>70</sub> -I <sub>76</sub>	

Note: that the BDW 2 should be transmitted before every back azimuth function. Slots for BDW 2 are reserved.

Note: also that if the flare function length would have been 5.9 msec, only 0.6 msec greater, a flare slot could contain an ADW and the data rate could be greater.

## Appendix B GPS timing and errors in pseudo ranges

In this section, the GPS time-of-transmission determination is described as well as some corrections needed to compensate for various errors. Also formulas for the calculation of the satellite positions are included. The information in this section was deduced from [3].

### B.1 Determining GPS time-of-transmission

The GPS-time is established by the Control Segment and has a zero point defined as midnight on the night of January 5, 1980/ morning of January 6, 1980. The longest unit used in stating the GPS-time is 1 week, defined as 604800 seconds.

In the navigation data every subframe contains a Hand-Over-Word (HOW), which contains the Time-Of-Week (TOW) word, which is a truncated version of the real TOW. That is: the HOW-TOW contains the 17 most significant bits of the real TOW. The TOW indicates the Z-count in one week. The Z-counter contains the total number of 'All ones'-epochs (X1-epochs) in the PRN code sequence from the beginning of the week. ( 403199 X1-epochs per week.)

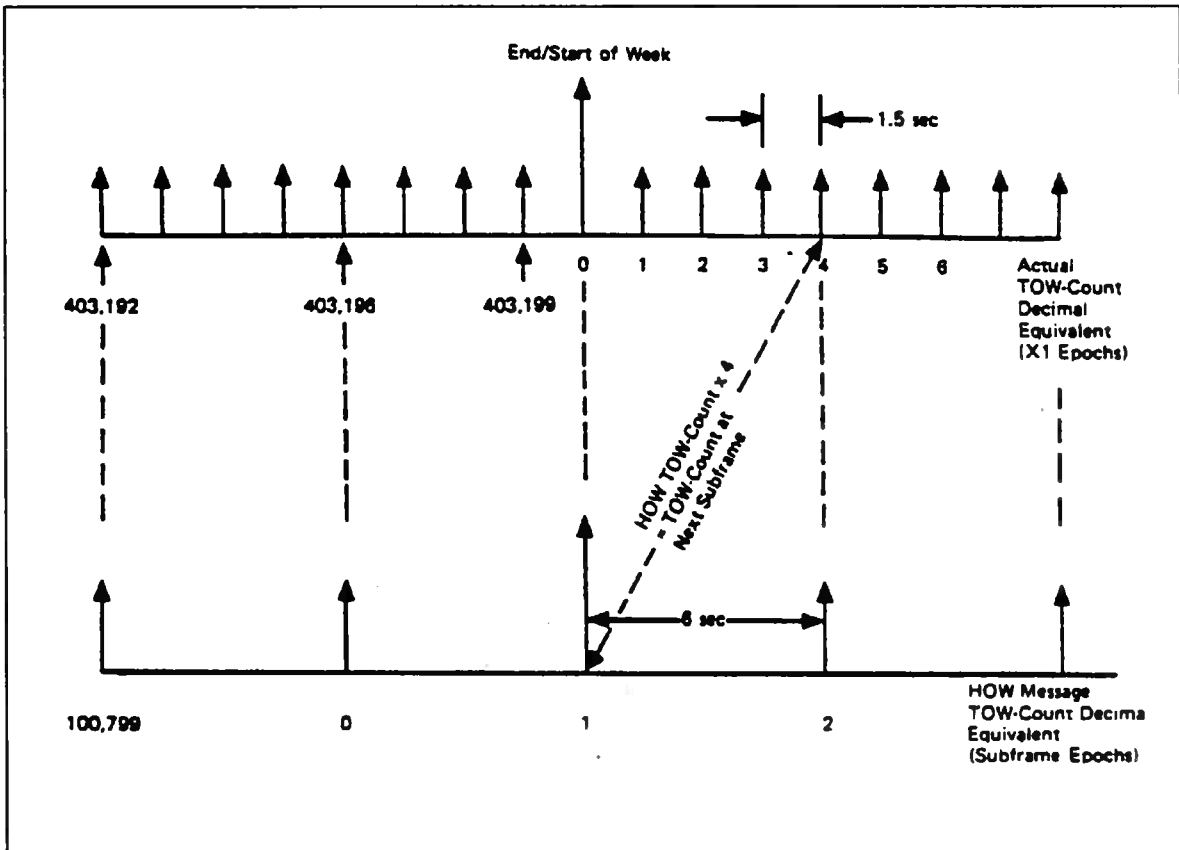


Figure B.1 Calculation of TOW from HOW-TOW

To calculate the real TOW from the HOW-TOW, the HOW-TOW should be multiplied by 4. The TOW as calculated with the HOW-TOW from one subframe, is the real TOW for the next subframe. See figure B.1 and [3, Appendix 2 to Annex A]. The time between two X1-epochs is 1.5 seconds, so the TOW can be calculated to a 6 second resolution. By counting the bits in the subframe, the resolution will be improved to 20 milliseconds ( 50 bit per second data-rate). Counting the complete PRN-codes that passed by in a data bit, the resolution is improved to 1 millisecond. The resolution is improved more by counting the chips in the 1023-chip PRN-code. The resolution will then be 1/1023 millisecond. By correlating the received code with the locally generated code, the resolution will be about 1% of 1/1023 millisecond. This equals about 3 meters.

The so called Selective Availability (SA) deteriorates the accuracy to about 100 m.

## *B.2 GPS time-of-transmission corrections*

The GPS receiver determines the time at which the GPS signals were transmitted. Because the satellite clock has an error, it does not indicate the standard GPS time. So the deviation of the satellite clock from the GPS time should be taken into account. Furthermore, corrections should be made for so called relativistic effects and effects caused by the rotation of the earth. This causes the indicated time to be different from the GPS time-of-transmission. Thus:

$$t = t_{SV} - \Delta t_{SV} \quad (B.1)$$

With 't' = GPS system time at the time of transmission(seconds)

't<sub>SV</sub>' = satellite time at the transmission time(seconds)

'Δt<sub>SV</sub>' = satellite time offset (seconds).

See figure B.2.

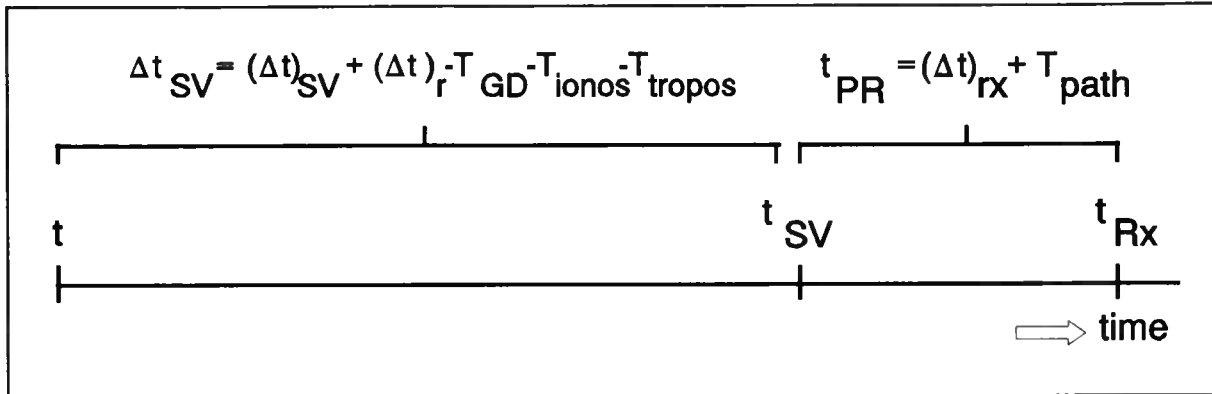


Figure B.2 Time axis for GPS pseudorange measurements

Where 't' is the indicated time of transmission, 't<sub>SV</sub>' is the corrected time of transmission, 't<sub>RX</sub>' is the reception time, '(Δt)<sub>SV</sub>' is the satellite clock error, '(Δt)<sub>r</sub>' is the relativistic error, 'T<sub>GD</sub>' is the L1-L2 correction, 'T<sub>ionos</sub>' and 'T<sub>tropos</sub>' are ionospheric and tropospheric corrections, '(Δt)<sub>RX</sub>' is the receiver clock error and 'T<sub>path</sub>' is the propagation delay of the radio signals if there were no errors.

### B.2.1 Satellite-clock correction

The indicated time-of-transmission is corrected for satellite clock errors by:

$$(\Delta t_{SV})_{SVck} = a_{f0} + a_{f1} \cdot (t - t_{oc}) + a_{f2} \cdot (t - t_{oc})^2 \quad (B.2)$$

With: 'a<sub>fx</sub>' are the coefficients of the polynomial, that describes the clock error. They are given in subframe 1 of the GPS message. With 'a<sub>f0</sub>' in (seconds), 'a<sub>f1</sub>' in (seconds/second) and 'a<sub>f2</sub>' in (seconds/ second<sup>2</sup>).

't<sub>oc</sub>' = the reference time for the clock corrections (second). 't<sub>oc</sub>' is transmitted also in subframe 1 of the GPS message.

From this it follows:

$$t = t_{SV} - (a_{f0} + a_{f1} \cdot (t - t_{oc}) + a_{f2} \cdot (t - t_{oc})^2) \quad (B.3)$$

As can be seen, this equation is coupled by the variable 't'. This means that to calculate 't', one needs to know 't'. This is not possible, but [3] indicates, that the sensitivity of 't<sub>SV</sub>' to 't' is negligible. That is why 't<sub>SV</sub>' can be used instead of 't' in (B.3). From this it follows:

$$t = t_{SV} - (a_{f0} + a_{f1} \cdot (t_{SV} - t_{oc}) + a_{f2} \cdot (t_{SV} - t_{oc})^2) \quad (B.4)$$

So:

$$(\Delta t_{SV})_{SVck} = a_{f0} + a_{f1} \cdot (t_{SV} - t_{oc}) + a_{f2} \cdot (t_{SV} - t_{oc})^2 \quad (B.5)$$

Note: If 't-t<sub>oc</sub>' is greater than 302400, 604800 should be subtracted from 't-t<sub>oc</sub>'. If 't-t<sub>oc</sub>' is smaller than -302400, 604800 should be added to 't-t<sub>oc</sub>', because of trespassing the beginning or the end of the week.

## B.2.2 Relativistic effects

Because of relativistic effects, the time-of-transmission as it is transmitted by the satellite will be different from the actual transmission time.

So:

$$(\Delta t_{SV})_{SVck+r} = (\Delta t_{SV})_{SVck} + (\Delta t)_r \quad (B.6)$$

Where  $(\Delta t)_r$  is:

$$(\Delta t)_r = F \cdot e \cdot \sqrt{A} \cdot \sin(E_k) \quad (B.7)$$

' $(\Delta t)_r$ ' = the relativistic correction term in (seconds).

'F' = a constant with value  $-4.442807633 \cdot 10^{-10}$  (seconds/ meter<sup>1/2</sup>). (This is deducted from the WGS-84 value for the gravitational constant of the earth.)

'e' = the eccentricity of the satellite orbit (dimensionless).

'A' = half long axis of the satellite orbit (meter).

'e' and 'A' are given in subframe 2 of the GPS message.

'E<sub>k</sub>' = the eccentric anomaly of the satellite orbit. This is calculated in the following intermezzo.

INTERMEZZO : Calculation of 'E<sub>k</sub>', the eccentric anomaly

The satellite orbit is described by a Kepler formula. Because the orbit of a satellite is not a perfect ellipse, there will be deviations from the ellipse. 'E<sub>k</sub>' describes the deviations of the eccentricity of the true satellite orbit to the eccentricity of the Kepler orbit. The eccentricity of the Kepler orbit is the variable 'e' in the GPS message (subframe 2 en 3).

The orbit of the satellite is defined so, that the satellite starts moving at GPS time 't<sub>oe</sub>' with a deviation of the ellipse orbit of 'M<sub>0</sub>'. The deviation will change as a function of time. This deviation is linear with time, with rate 'n'. The rate 'n' is determined by a constant 'n<sub>0</sub>', which is determined by the gravitation of the earth, and a deviation 'Δn'. 'Δn' is caused among others by the gravitation of other celestials.

'E<sub>k</sub>' is given by the equation of Kepler:

$$M_k = E_k - e \cdot \sin(E_k) \quad (\text{B.8})$$

In [10] these equations are mentioned. This formula is coupled by the variable 'E<sub>k</sub>', which should be calculated. Rewriting this formula gives:

$$E_k = M_k + e \cdot \sin(E_k) \quad (\text{B.9})$$

This formula can be solved by iteration. The starting value is: 'E<sub>k</sub>' = 'M<sub>k</sub>' ('M<sub>k</sub>' = mean anomaly). The iteration is stopped when 'E<sub>k</sub>[n+1]' does not deviate more than 'ε' from 'E<sub>k</sub>[n]', with 'n' is the number of iterations.

'M<sub>k</sub>', the mean anomaly of the eccentricity of the satellite orbit from the Kepler orbit can be calculated as follows:

$$M_k = M_0 + n \cdot t_k \quad (\text{B.10})$$

With: 'M<sub>0</sub>' = mean deviation at the reference time (radians). 'M<sub>0</sub>' is the deviation of the eccentricity at the moment 't<sub>k</sub>' = 0, when the ephemeris parameters became valid. See subframe 2 en 3 and [3].

'n' = Corrected mean motion (speed of the eccentricity-deviation).

't<sub>k</sub>' = time from the ephemeris reference time.

' $t_k$ ' is given by:

$$t_k = t - t_{oe} \quad (\text{B.11})$$

With: ' $t_{oe}$ ' = the reference time of the ephemeris data.  $t_{oe}$  is given in subframe 2.

' $t$ ' = GPS time.

And ' $n$ ' is given by:

$$n = n_0 + \Delta n \quad (\text{B.12})$$

With: ' $\Delta n$ ' = The mean deviation of the motion of the satellite in (radians/ second) compared to the calculated value. See subframe 2 en 3.

' $n_0$ ' = calculated mean motion (the rate of the eccentricity-deviation)

Note: in the GPS ephemeris, ' $\Delta n$ ' is given in (semicircles/second).

' $n_0$ ' is given by:

$$n_0 = \sqrt{\frac{\mu}{A^3}} \quad (\text{B.13})$$

With: ' $\mu$ ' = the gravitation constant of the earth according to WGS-84. This value is:  $3.986005 \cdot 10^{14}$  (meter<sup>3</sup>/ second<sup>2</sup>).

END OF INTERMEZZO

### B.2.3 L1-frequency correction

When only the L1-frequency is used, ' $t$ ' from (B.6) should be corrected for errors caused by group delay.

$$(\Delta t_{SV})_{SV_{ck+r+L1}} = (\Delta t_{SV})_{SV_{ck+r}} - T_{GD} \quad (\text{B.14})$$

With ' $T_{GD}$ ' = group delay correction for L1 and L2. It is calculated to account for satellite group delay differences between L1 and L2 based on measurements made by the satellite manufacturer. ' $T_{GD}$ ' is transmitted in subframe 1.

From this it follows with (B.6):

$$t = t_{SV} - ((\Delta t_{SV})_{SV_{ck}} + (\Delta t)_r - T_{GD}) \quad (\text{B.15})$$

Time ' $t$ ', which is calculated now, is the GPS time of the transmission. It should be corrected for ionospheric and tropospheric errors.

## B.2.4 Ionospheric corrections

In [3, appendix 6], a correction model for ionospheric errors is listed. The ' $T_{ionos}$ ' which is calculated with this model represents the delay of the signal in the ionosphere. From this it follows that the signal comes late, so ' $\Delta t_{SV}$ ' must become smaller.

It follows:

$$(\Delta t_{SV})_{SVck+r+LI+ionos} = (\Delta t_{SV})_{SVck+r+LI} - T_{ionos} \quad (B.16)$$

So:

$$t = t_{SV} - ((\Delta t_{SV})_{SVck} + (\Delta t_r) - T_{GD} - T_{ionos}) \quad (B.17)$$

## B.2.5 Tropospheric corrections

The same reasoning that led to the ionospheric correction, will lead to the troposphere correction. So

$$(\Delta t_{SV})_{SVck+r+LI+ionos+tropos} = (\Delta t_{SV})_{SVck+r+LI+ionos} - T_{tropos} \quad (B.18)$$

So:

$$t = t_{SV} - ((\Delta t_{SV})_{SVck} + (\Delta t_r) - T_{GD} - T_{ionos} - T_{tropos}) \quad (B.19)$$

## *B.3 Satellite position calculations and pseudo range correction*

### B.3.1 Satellite-position calculation

With the time 't', which was deducted above, the satellite position can be calculated. This process is described in [3] and a copy of the formulas is shown now.

GPS SATELLITE POSITION CALCULATIONS

$$\mu = 3.986005 \times 10^{14} \frac{\text{meter}^3}{\text{sec}^2} \quad (\text{B.20})$$

' $\mu$ ' is the WGS-84 value of the Earth's Universal Gravitational Constant.

$$\dot{\Omega}_e = 7.2921151467 \times 10^{-5} \frac{\text{rad}}{\text{sec}} \quad (\text{B.21})$$

' $\Omega$ ' is the WGS-84 value of the Earth's rotation rate.

$$A = [\sqrt{A}]^2 \quad (\text{B.22})$$

'A' is the Semi-Major Axis.

$$n_o = \sqrt{\frac{\mu}{A^3}} \quad (\text{B.23})$$

' $n_o$ ' is the Computed Mean Motion.

$$t_k = t - t_{oe} \quad (\text{B.24})$$

't' is the Time from Ephemeris Reference Epoch.

$$n = n_o + \Delta n \quad (\text{B.25})$$

'n' is the Corrected Mean Motion.

$$M_k = M_o + n \cdot t_k \quad (\text{B.26})$$

' $M_k$ ' is the Mean Anomaly.

$$M_k = E_k - e \cdot \sin(E_k) \quad (\text{B.27})$$

Kepler's Equation for Eccentric Anomaly, to be solved iteratively.

$$v_k = \text{atan}\left(\frac{\sin(v_k)}{\cos(v_k)}\right) = \text{atan}\left(\frac{\sqrt{1-e^2} \cdot \sin(E_k)}{\cos(E_k) - e}\right) \quad (\text{B.28})$$

' $v_k$ ' is the True Anomaly.

$$\Phi_k = \nu_k + \omega \quad (B.29)$$

' $\Phi_k$ ' is the Argument of Latitude.

$$\begin{aligned} \delta u_k &= C_{us} \cdot \sin(2\Phi_k) + C_{uc} \cdot \cos(2\Phi_k) \\ \delta r_k &= C_{rc} \cdot \cos(2\Phi_k) + C_{rs} \cdot \sin(2\Phi_k) \\ \delta i_k &= C_{ic} \cdot \cos(2\Phi_k) + C_{is} \cdot \sin(2\Phi_k) \end{aligned} \quad (B.30)$$

' $\delta u_k$ ' is the Argument of Latitude Correction for Second harmonic perturbations.

' $\delta r_k$ ' is the Radius Correction for Second harmonic perturbations.

' $\delta i_k$ ' is the Correction to Inclination for Second harmonic perturbations.

$$u_k = \Phi_k + \delta u_k \quad (B.31)$$

' $u_k$ ' is the Corrected Argument of Latitude.

$$r_k = A \cdot (1 - e \cdot \cos(E_k)) + \delta r_k \quad (C.1)$$

' $r_k$ ' is the Corrected Radius.

$$i_k = i_o + \delta i_k + IDOT \cdot t_k \quad (C.2)$$

' $i_k$ ' is the Corrected Inclination.

'IDOT' is the Rate of Inclination angle.

$$\begin{aligned} x_k &= r_k \cdot \cos(u_k) \\ y_k &= r_k \cdot \sin(u_k) \end{aligned} \quad (C.3)$$

' $x_k$ ' and ' $y_k$ ' is the position in the Orbital Plane.

$$\Omega_k = \Omega_o + (\dot{\Omega} - \dot{\Omega}_e) \cdot t_k - \dot{\Omega}_e \cdot t_{oe} \quad (C.4)$$

' $\Omega$ ' is the Corrected Longitude of Ascending Node.

$$\begin{aligned} x_k &= x_k \cdot \cos(\Omega_k) - y_k \cdot \cos(i_k) \sin(\Omega_k) \\ y_k &= x_k \cdot \sin(\Omega_k) + y_k \cdot \cos(i_k) \cos(\Omega_k) \\ z_k &= y_k \cdot \sin(i_k) \end{aligned} \quad (C.5)$$

' $x_k$ ', ' $y_k$ ' and ' $z_k$ ' are the Earth Centred Earth Fixed (ECEF) coordinates.

#### END OF GPS SATELLITE POSITION CALCULATIONS

**Note: the formulas in the [3] and the previous page are meant for parameters which are in radians. The ephemeris parameters in the GPS message are (mostly) in semicircles. 1 semicircle is 3.1415926535898 radians.<sup>1</sup>**

Besides the listed calculations, the earth rotation during the propagation time of the radio-signal should be accounted for. The travel time of the signal is approximated as follows:

$$TRAVEL = \frac{PSEUDO\ RANGE}{C} - CLOCKOFFSET_{user} \quad (C.6)$$

The rotation-rate of the earth is found by multiplying the earth angular rotation-rate by the signal travel time.

$$\alpha = TRAVEL \cdot 7.2921151467 \cdot 10^{-5} \frac{rad}{s} \quad (C.7)$$

The position of all satellites used in the position calculation can now be corrected with the following formula.

Where (X,Y,Z) is the original satellite position and (X',Y',Z') is the corrected satellite position.

---

<sup>1</sup> This number  $\pi$  is different from the number  $\pi$  defined in WGS-84.  $\pi$  is just a mathematical constant.

$$\begin{bmatrix} X' \\ Y' \\ Z' \end{bmatrix} = \begin{bmatrix} \cos(\alpha) & \sin(\alpha) & 0 \\ -\sin(\alpha) & \cos(\alpha) & 0 \\ 0 & 0 & 1 \end{bmatrix} \cdot \begin{bmatrix} X \\ Y \\ Z \end{bmatrix} \quad (C.8)$$

### B.3.2 Pseudo range correction

To calculate the pseudorange, the reception time 't<sub>r</sub>', which is given by the receiver, should be decreased with the transmission time 't', which is calculated above. The result is then multiplied by the speed of light.

So:

$$PR = (t_{rx} - (t_{SV} - ((\Delta t_{SV})_{SVck} + (\Delta t)_r - T_{GD} - T_{ionos} - T_{tropos}))) \cdot c \quad (C.9)$$

When brackets are deleted, it follows:

$$PR = (t_{rx} - t_{SV} + (\Delta t_{SV})_{SVck} + (\Delta t)_r - T_{GD} - T_{ionos} - T_{tropos}) \cdot c \quad (C.10)$$

Note: These pseudo ranges are not corrected for the receiver clock error.

Note: Receiver noise and multipath also deteriorate the range measurements.

### B.4 Position calculation

The equations derived in section B.3.2 represent the radii of spheres around the satellites at which the user is located, plus the user clock error.

With the satellite positions and pseudo ranges, the user position can be calculated. At the same time the receiver clock error is calculated as well. The position and the receiver clock error are calculated using a linearised version of the following minimum set of equations:

$$\begin{aligned} \sqrt{(x-x_1)^2 + (y-y_1)^2 + (z-z_1)^2} + c \cdot \Delta t_{rx} &= PR_1 \\ \sqrt{(x-x_2)^2 + (y-y_2)^2 + (z-z_2)^2} + c \cdot \Delta t_{rx} &= PR_2 \\ \sqrt{(x-x_3)^2 + (y-y_3)^2 + (z-z_3)^2} + c \cdot \Delta t_{rx} &= PR_3 \\ \sqrt{(x-x_4)^2 + (y-y_4)^2 + (z-z_4)^2} + c \cdot \Delta t_{rx} &= PR_4 \end{aligned} \quad (C.11)$$

Where (X,Y,Z) is the receiver antenna position and (X<sub>a</sub>,Y<sub>z</sub>,Z<sub>a</sub>) is the position of satellite 'a'.

The calculated receiver-clock error 'Δt<sub>rx</sub>' has to be used to correct 't<sub>rx</sub>' until it indicates the GPS-time in the receiver. See formula (C.12).

Note: that 'Δt<sub>rx</sub>' should not be used to correct 't<sub>SV</sub>'.

$$(t_{rx})_{new} = (t_{rx})_{old} - \Delta t_{rx} \quad (C.12)$$

So the correction algorithm is like this:

- 1) correct the transmission time for satellite clock error
- 2) correct the transmission time for relativistic effects
- 3) correct the transmission time for group delays
- 4) correct the transmission time for ionospheric delay
- 5) correct the transmission time for tropospheric delay
- 6) do 1 iteration to calculate the position-corrections and receiver clock-error
- 7) if the receiver clock error > allowed error, or  
if the position correction > allowed error, go to 6,
- 8) the position is correct, the receiver clock indicated the GPS time.

Figure B.3 shows this algorithm as it is shown in [3].

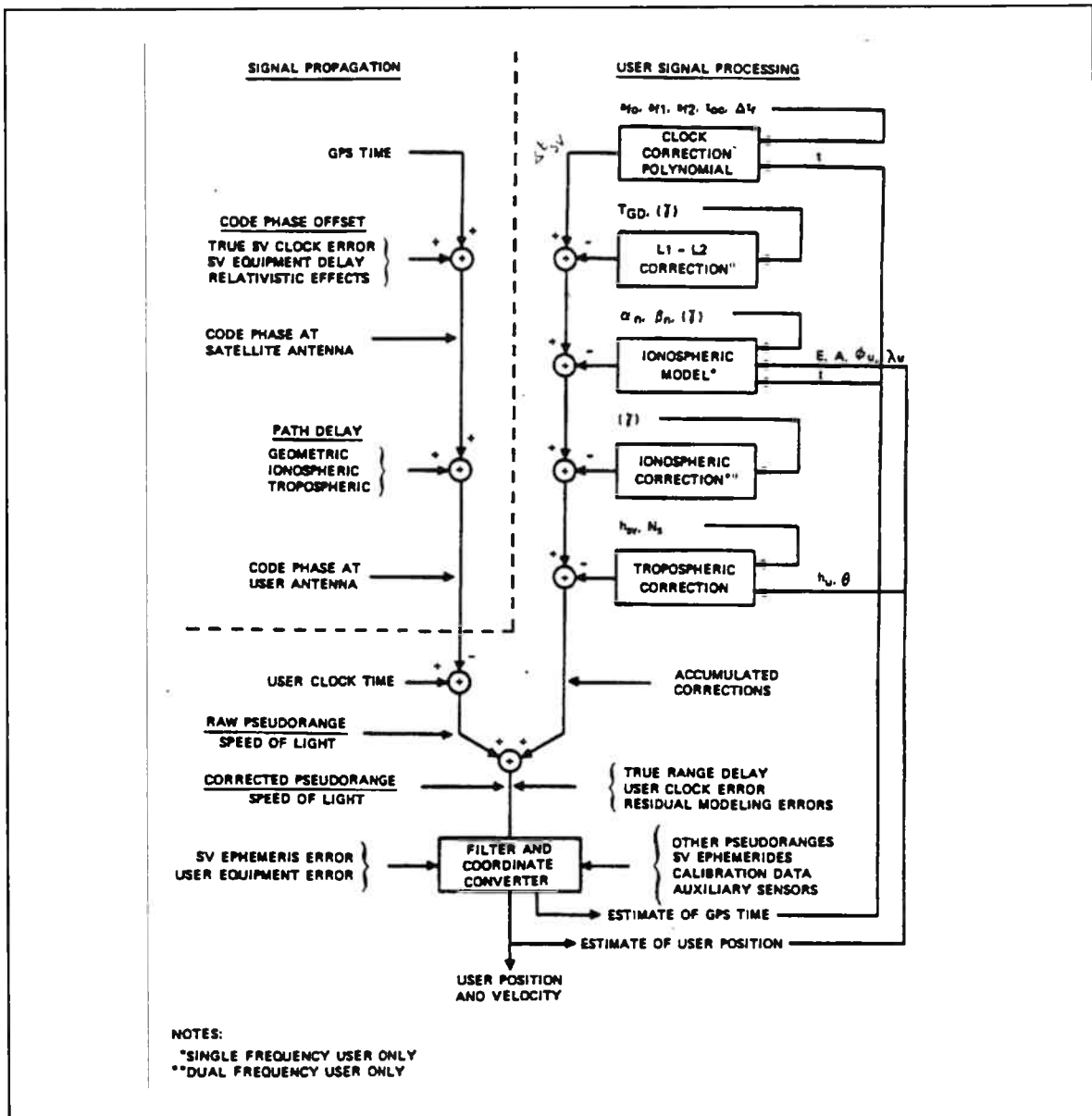


Figure B.3 GPS positioning according to STANAG

## Appendix C Errors caused by asynchronicity of information

### C.1 Introduction

In this section, the errors in MIAS are considered, which occur when a position is calculated at a certain time with partly old information, because of asynchronicity.

In the MIAS system MLS, DME, GPS and possibly attitude information are not synchronised. Figure C.1 shows a time axis, where the information arrival time for MLS and GPS is depicted relative to each other.

The longest delay between MLS and GPS information is  $1/39$  (s) for elevation information and  $1/13$  (s) for azimuth information.

Extrapolating information is a possibility to handle the asynchronicity of the signals, but it will be more difficult than just remembering the old value of one of the sensors.

Apart from being difficult, the knowledge and software for extrapolating noisy signals is not available yet.

Special application of the Kalman filter makes it possible to use asynchronous inputs, which could even have some advantages over synchronous inputs. See [19] for more information about Kalman filters.

### C.2 Flight situations considered for error calculation

Now four flight situations are considered in order to calculate the errors which are made when using old information.

Four speed directions are distinguished. Direction A has a direction perpendicular to the line through the azimuth transmitter and the aircraft. Direction B has a speed along the runway centreline.

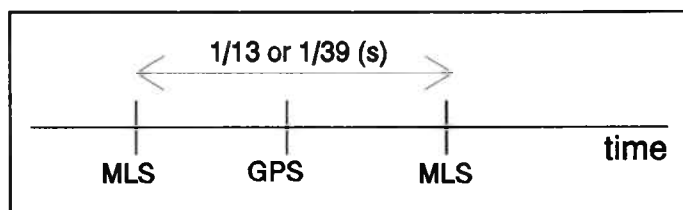


Figure C.1 MIAS time axis

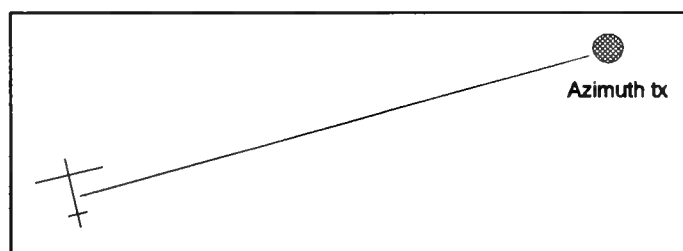


Figure C.2 Direction A

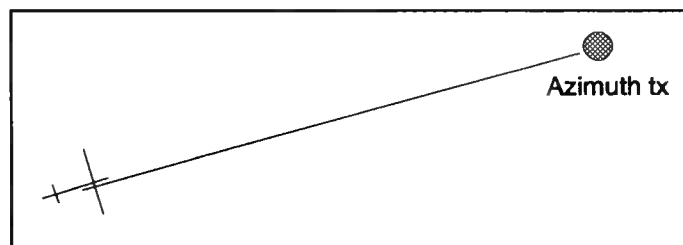


Figure C.3 Direction B

(see figure C.2 and C.3). Direction C has a direction perpendicular to the line through the elevation transmitter and the aircraft. Direction D has a direction along the line through the elevation transmitter and the aircraft (see figure C.4 and C.5).

NOTE: In the following calculations planar scanning beams will be used for MLS. Most usual are conical scanning beams. The latter are more difficult to calculate and the results won't differ (much).

### C.3 Azimuth error

Suppose the distance between the azimuth transmitter and the aircraft is 1000 (m), a typical runway length. Furthermore, the aircraft is flying with a speed of 100 (m/s) in direction A.

The position error for azimuth in 1/13 (s) is  $100 * 1/13 = 7,69$  (m). From this, it follows (using figure C.6) that  $\Delta Az = 2 * \text{atan}(7,69 / 2 * 1000)$ , from which it follows:  $\Delta Az = 0,44^\circ$ .

If the aircraft flew in direction B, no angular error is made.

### C.4 Elevation error

For the calculation of the error in elevation, a different assumption is used:

the direction of the speed of the aircraft is direction C. If we take the true speed to be 100 (m/s) and the distance between the elevation transmitter and the aircraft 100 (m), a typical distance between the runway threshold and the elevation transmitter.

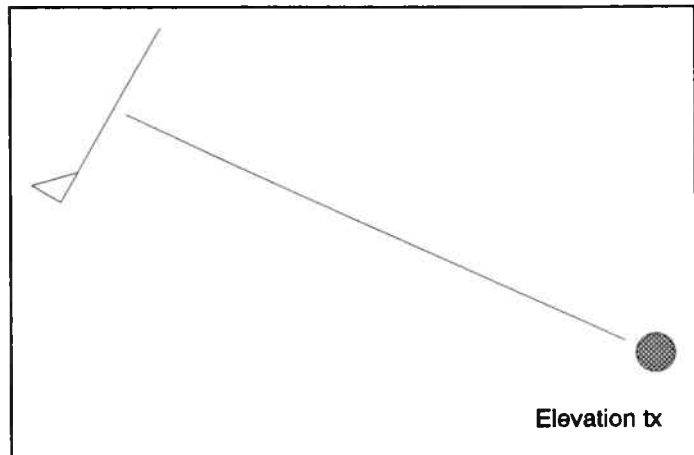


Figure C.4 Direction C

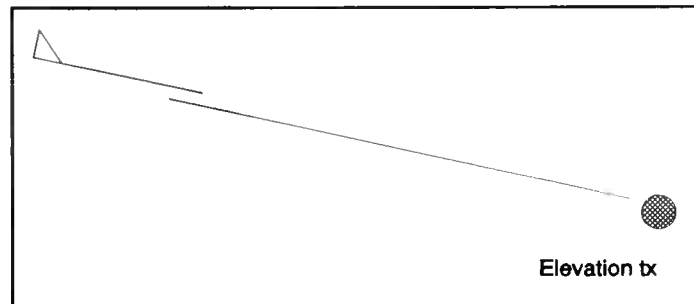


Figure C.5 Direction D

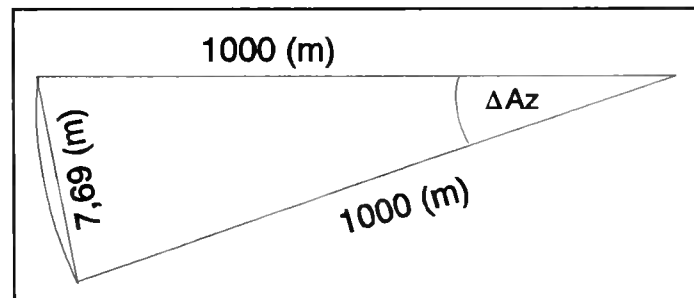


Figure C.6 Azimuth calculation

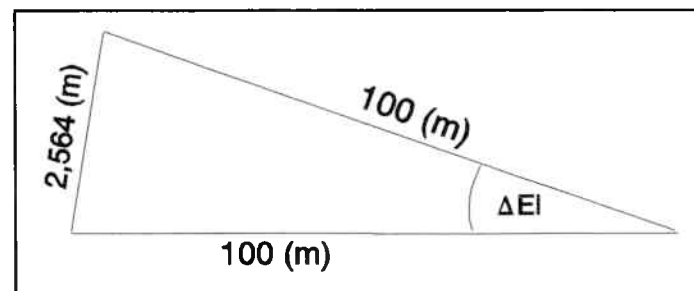


Figure C.7 Elevation calculation

The position error for elevation in 1/39 (s) is  $100 * 1/39 = 2,564$  (m). From this, it follows (using figure C.7) that  $\Delta E1 = 2 * \text{atan}(2,564 / 2 * 100)$ , from which it follows:  $\Delta E1 = 1,468^\circ$ .

If the aircraft flew in direction D, no error is made.

### C.5 Realistic errors

If the Azimuth transmitter is placed along the runway centreline, then using a speed in direction A will give the worst angle error. But direction A won't occur during landing. For landing, direction B will be normal and the angular error then will be zero.

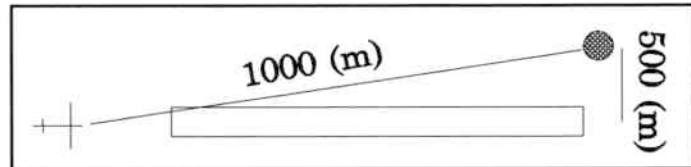


Figure C.8 Computed centreline

#### C.5.1 Azimuth realistic error

If the Azimuth transmitter is offset the centreline (computed centre line approach, see figure C.8), the angular error for final approach will be a fraction of the angle error with direction A.

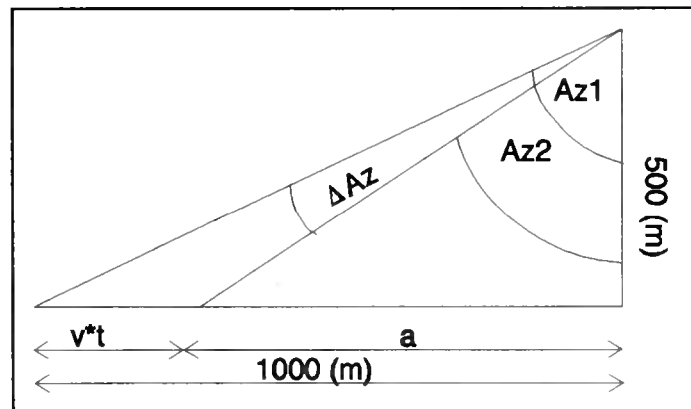


Figure C.9 Calculate  $\Delta Az$

For this calculation, see figure C.8. The azimuth offset is assumed to be 500 (m) ([2] allows coding of Azimuth transmitter offset of 511 (m)) and the azimuth to threshold distance is 1000 m. If figure C.8 is abstracted, figure C.9 results. The length of line a is:  $1000 - v*t = 1000 - 7.69 = 992.31$  (m). From this  $Az1$  and  $Az2$ , which difference is the Azimuth error angle, can be calculated.

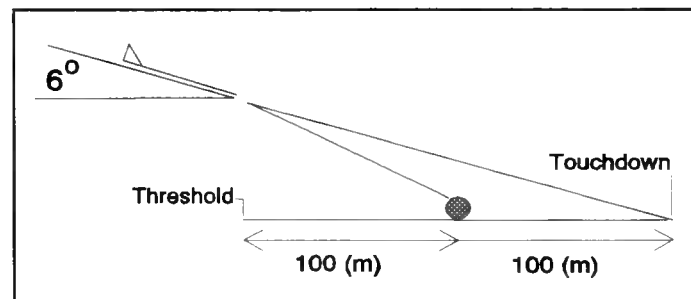


Figure C.10 Computed Elevation

$\text{Tan}(Az1) = (1000/\text{off})$  and  $\text{Tan}(Az2) = (a/\text{off})$ .  $\Delta Az = Az1 - Az2 = 63.4349 - 63.2576 = 0,1773^\circ$ .

### C.5.2 Elevation realistic error

The Elevation angle error calculated above for direction C is a very pessimistic error, because in the final approach, the aircraft won't be flying in direction C. More likely it will fly in a direction as shown in figure C.10, where a  $6^\circ$  glideslope and a touchdown 100 m beyond the elevation transmitter is depicted. The elevation transmitter is at

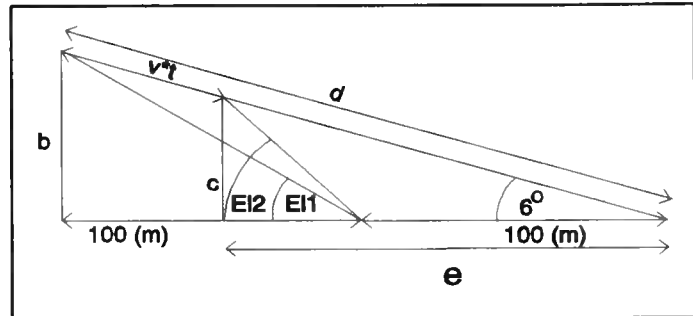


Figure C.11 Calculate  $\Delta El$

100 m from the threshold. This figure can be abstracted to figure C.11. From this, distance b, c, d and e can be calculated.  $B = 200 \cdot \tan(6^\circ) = 21,021$  (m),  $d = 200 / \cos(6^\circ) = 201,102$  (m),  $c = \sin(6^\circ) \cdot (d - v \cdot t) = 20,753$  (m) and  $e = c / \tan(6^\circ) = 197,450$  (m). From these figures it follows that  $El_1 = \text{atan}(b/100) = 11,871^\circ$  and  $El_2 = \text{atan}(c/(e-100)) = 12,022^\circ$ . This make  $\Delta El = 0,151^\circ$ .

### C.6 Conclusion

Using old MLS information for calculating the position with a hybrid system in a normal approach (azimuth on extended centre-line and a glidepath towards the elevation transmitter), will introduce errors that are zero degrees in elevation and azimuth at the threshold. The along track error will be significant.

Other situations will give errors of less than  $0,16^\circ$  for Elevation and less than  $0,18^\circ$  for Azimuth. These errors are small and can be calculated using the speed and course of the aircraft, and the distance to the azimuth and elevation transmitters.

## Appendix D The metric error caused by an angular error

This appendix describes the metric error caused by an error in the angle measurement. This is proven with an example in 2-D.

Suppose an angle ' $\alpha$ ' is measured in a point 'O'. The angle measurement has an error expressed in radians ' $d\alpha$ '. The angular error causes a metric error, because of the distance 'R'. Figure D.1 shows the point 'O', the distance 'R', the true angle ' $\alpha$ ' and the angular error ' $d\alpha$ '.

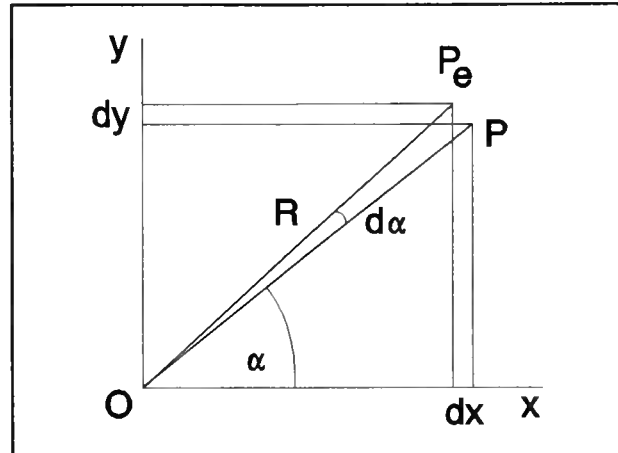


Figure D.1 The metric error caused by an angular error.

The true position 'P' is:

$$P=[R \cdot \cos(\alpha), R \cdot \sin(\alpha)] \quad (D.1)$$

The erroneous position 'P<sub>e</sub>' is:

$$P_e=[R \cdot \cos(\alpha + d\alpha), R \cdot \sin(\alpha + d\alpha)] \quad (D.2)$$

The error in the x and y direction, 'dx' and 'dy' is then:

$$\begin{aligned} dx &= R \cdot \cos(\alpha + d\alpha) - R \cdot \cos(\alpha) \\ dy &= R \cdot \sin(\alpha + d\alpha) - R \cdot \sin(\alpha) \end{aligned} \quad (D.3)$$

This can be expanded to:

$$\begin{aligned} dx &= R(-2\sin\frac{1}{2}(\alpha + d\alpha + \alpha)\sin\frac{1}{2}(\alpha + d\alpha - \alpha)) = R(-2\sin(\alpha + \frac{1}{2}d\alpha)\sin(\frac{1}{2}d\alpha)) \\ dy &= R(2\sin\frac{1}{2}(\alpha + d\alpha - \alpha)\cos\frac{1}{2}(\alpha + d\alpha + \alpha)) = R(2\sin(\frac{1}{2}d\alpha)\cos(\alpha + \frac{1}{2}d\alpha)) \end{aligned} \quad (D.4)$$

The metric error 'dm' is:

$$dm = \sqrt{dx^2 + dy^2} \quad (D.5)$$

Using 'dx' and 'dy' from formula D.4, the following formula results:

$$dm = \sqrt{R^2(4\sin^2(\alpha + \frac{1}{2}d\alpha)\sin^2(\frac{1}{2}d\alpha) + 4\sin^2(\frac{1}{2}\alpha)\cos^2(\alpha + \frac{1}{2}d\alpha))} \quad (D.6)$$

Which can be simplified to:

$$dm = 2R\sin(\frac{1}{2}d\alpha) \sqrt{\sin^2(\alpha + \frac{1}{2}d\alpha) + \cos^2(\alpha + \frac{1}{2}d\alpha)} \quad (D.7)$$

$$dm = 2R\sin(\frac{1}{2}d\alpha) \cdot 1 \quad (D.8)$$

If the angle 'dα' is small, 'dm' can be written as shown in the following formula:

$$dm \approx 2R \cdot \frac{1}{2}d\alpha \quad (D.9)$$

The result is:

$$dm \approx R d\alpha \quad (D.10)$$

for small angular errors.

It can be concluded from formula D.10, that for small errors, the position error relative to the origin is linearly dependent on the angular error 'dα' and on the error in 'R'.

## **Appendix E MAGNAVOX MX4200D messages for MIAS**

This section lists the messages used to program the MX4200D and the messages used by the MIAS computer to extract GPS information. The communication with the GPS receiver is via two EIA RS-422 channels. The specifications for the connections and baud rates are listed at the end of this section.

### *E.1 Messages for programming the MX4200D*

The MX4200D can be programmed with some operating parameters using the control channel (port 0). The parameters used by the MIAS program are:

- the horizontal acceleration factor, which determines the bandwidth of the positioning filter,
- the elevation limit, which eliminates the use of satellites under a elevation angle, and
- time recovery, which assures that receiver time will indicate the GPS time.

Furthermore, the MX4200D can be programmed to output or cancel outputting certain data fields. It can be ordered to output ephemeris and almanac instantly or to reset itself. The initialising parameters are used to simplify the acquisition of the satellites.

Table E.1 lists the messages, their labels and the structure which are used to program the GPS MX4200D.

### *E.2 Message used for retrieving GPS information*

The MX4200D sends raw GPS data via the raw data channel (port 1). This includes:

- transmission and reception times, integrated carrier phase, and code offset for calculating pseudoranges
- GPS messages from subframes 1 to 5. These include ephemeris to calculate satellite positions, and satellite clock correction parameters, and ionospheric correction parameters. The GPS message is coded by the MX4200D as hexadecimal numbers each representing 8 bits of a subframe. The subframes coding can be found in [3].

The message label and structure of the raw data messages are listed in table E.2.

The MIAS program also 'listens' to the control channel for one message indicating the number of satellites being tracked. The structure of this label is listed in table E.3.

### *E.3 MX4200D to computer connections*

The MX4200D has four output channels using the EIA RS-422 protocol. The control channel (port 0) uses the NMEA-0183 protocol, see [20], at 4800 Bits per second and the raw data channel (port 1) uses a Magnavox protocol also at 4800 Bits per second. Both channels use ASCII coding with 8 databits, 1 stopbit and no parity. The bitrate can be changed. There are two more output channels which are not used.

Both channels used are available on a single female D-25 connector. The pin-layout of the female D-25 connector is listed in table E.4. The two used output-channels are connected to a RS-422 extension board, which has a female D-37 connector. The pin-layout of this connector is listed in table E.5. In table E.6, the connections between the MX4200D and the RS-422 card are listed.

Note: that the MX4200D outputs should be connected to the RS-422 inputs.

Table E.1 Magnavox MX4200D program messages

Record number	Field	Field contents	Range	
\$PMVXG,000	DD	Day of Month	1-31	
	MM	Month of Year	1-12	
	YYYY	Year	1991-9999	
	HHMMSS	GMT	0-235959	
	DDMM.MMMM	Latitude( deg, min)	0-89.9999	
	N	North( S= South)	N or S	
	DDDMM.MMMM	Longitude( deg, min)	0-179.9999	
	W	West( E= East)	E or W	
	HHHHH.H	Altitude (height above mean sea level) (m)	0-99999.9	
	X	Not used		
\$PMVXG,001	X	Constrain altitude:           0: never;           1: auto 2: always;           3: coast	0-3	
	X	Not used		
	X.XX	Horizontal acceleration factor (m/s <sup>2</sup> )	0.5-10.0	
	X	Not used		
	XXXX	VDOP limit	1-9999	
	XXXX	HDOP limit	1-9999	
	XX	Elevation limit	0-90	
	X	Time output mode           U: UTC; L: Local time	U,L	
	HHHMM	Local time offset (±) from GMT	+0-2359	
	\$PMVXG,018	X	Reset type:                   W: Warm start;    C: Cold start T: Tepid start	C,W,T
\$PMVXG,023		X	Time recovery mode: D: Dynamic;                   S: Static; K: Known position;           N: No time recovery	D,S,K,N
		X	Time synchronisation:       U: UTC;            G: GPS	U,G
	X	Time Mark Mode:           A: Always;        V: Only when valid	A,V	
\$PMVXG,024	XXXX	Maximum time error in nanoseconds	50-1000	
	XXXXX	User Time Bias	+0-99999	
	X	ASCII message ctrl:       0: no output;     1: output to ctrl port 2: output to equi port	0-2	
	X	Know position prn:           0: turn off single satellite mode	0-37	
	X	Nav Results:	+,-	
	X	Raw Measurements:	+,-	
	X	Almanac & Ephemeris:	+,-	
	X	Constellation info:	+,-	
	X	Time Recovery:	+,-	
	X	Full Debug:	+,-	
\$PMVXG,027	X	Partial Debug:	+,-	
	XXXXX	Not known	3-6,8-11	
	X	Raw measurement compression ctrl: 0: ASCII;           1: Compressed only 2: Both	0-2	
X	Almanac/Ephemeris request: 0: Output almanac data now 1: Output ephemeris data now 2: Output almanac & ephemeris data now	0-2		

Table E.2 Magnavox MX4200D Raw-data output messages

Record number	Bytes	Identifier	Description	range
1	1-4	ID	Record ID	1
	6-7	CHNL	Receiver Channel nr	1-6
	9-10	PRN	Satellite PRN number	1-32
	12-20	USER_MS	User time of measurement (millisecond)	0-604799999
	22-30	CHNL_MS	Channel time of measurement (millisecond)	0-604799999
	32-41	PHI	Integrated carrier phase L1 wavelengths	
	43-48	CODE	Raw code offset L1 wavelengths	-128-127
	50-53	PHI_FRAC	Integrated carrier phase, fractional portion. LSB=(L1 wavelength)/256	
	55-58	CR	Costas ration	-128-127
	60-63	SNR	Signal-to-noise ratio at 1 Hz bandwidth. dB-Hz	25-53
	65		?: Phase ambiguity unknown +/-: Changing gives better resolution of phase measurement	-,+ ,?
200	1-4	ID	Record ID	200
	6-7	PRN	Satellite PRN number of following messages	1-32
201	1-4	ID	Record ID	201
	6-76	Subframe 1	Subframe 1 contents according to ICD-200 packed in 24 pairs of hex-ASCII digits. All parity's removed. TLM and HOW are not output	
202	1-4	ID	Record ID	202
	6-76	Subframe 2	id for subframe 2	
203	1-4	ID	Record ID	203
	6-76	Subframe 3	id for subframe 3	
100	1-4	ID	Record ID	100
	6-7	PRN	Satellite PRN number used for Almanac	1-32
101-132	1-4	ID	Record ID	101-132
	6-76	Almanac SV XX	Almanac data packed in 24 pairs of hex-ASCII digits. All parity's removed. TLM and HOW are not output. Subframe 5 page 1-24 and subframe 4 page 2,3,4,5,7,8,9,10	
133-134	1-4	ID	Record ID	133-134
	6-76	Health	Health data for satellites 1-32 subframe 4 page 25 and subframe 5 page 25	
135	1-4	ID	Record ID	135
	6-76	Ionospheric correction	Ionospheric correction parameters as in subframe 4 page 18	

Table E.6 MX4200D interconnection to RS-422 card

Pin number	MX4200 connector		Pin number	RS-422 card	
		Pin name			Pin name
2		B input +	2		Transmit Data + Ch1
14		B input -	20		Transmit Data - Ch1
3		B output +	3		Receive Data + Ch1
15		B output -	21		Receive Data - Ch1
6		C input +	11		Transmit Data + Ch2
18		C input -	30		Transmit Data - Ch2
8		C output +	12		Receive Data + Ch2
21		C output -	31		Receive Data - Ch2

Table E.3 Magnavox MX4200D control port output messages

Record number	Field	Field contents
\$PMVXG,000	XXX	Receiver status: ACQ: Satellite re-acquisition ALT: Constellation Selection IAC: Initial acquisition IDL: Idle, no satellites NAV: Navigation STS: Search the Sky TRK: Tracking
	XX	Number of Satellites that should be visible
	X	Number of Satellites being tracked
	HHMM	Time since last navigation
	X	Initialization status: 0: Waiting for initialisation 1: Initialisation complete

Table E.4 MX4200D pin numbers and pin names used in MIAS

Pin number	Pin name	Pin number	Pin name
1	not connected	14	B input -
2	B input +	15	B output -
3	B output +	16	not connected
4	not connected	17	not connected
5	not connected	18	C input -
6	C input -	19	not connected
7	not connected	20	not connected
8	C output +	21	C output -
9	not connected	22	not connected
10	not connected	23	not connected
11	not connected	24	not connected
12	not connected	25	not connected
13	not connected		

Table E.5 RS-422 connector pin numbers and pin names.

Pin number	Pin name	Channel	Pin number	Pin name	Channel
1	Ground	1	20	Transmit Data -	1
2	Transmit data +	1	21	Receive Data -	1
3	Receive data +	1	22	Request to Send -	1
4	Request to Send +	1	23	Clear to Send -	1
5	Clear to Send +	1	24	Data Set Ready -	1
6	Data Set Ready +	1	25	DCD -	1
7	Ground	1	26	Data Terminal Ready +	1
8	DCD +	1	27	Ring Indicator +	1
9	Data Terminal Ready -	1	28	Ground	-
10	Ring Indicator -	1	29	Ground	2
11	Transmit Data +	2	30	Transmit data -	2
12	Receive Data +	2	31	Receive Data -	2
13	Request to Send +	2	32	Request to Send -	2
14	Clear to Send +	2	33	Clear to Send -	2
15	Data Set Ready +	2	34	Data Set Ready -	2
16	Ground	2	35	DCD -	2
17	DCD -/+?	2	36	Data Terminal Ready +	2
18	Data Terminal Ready -	2	37	Ring Indicator +	2
19	Ring Indicator -	2			

## Appendix F Bendix MLS 20-A connections to CDU and MIAS computer

In this section the connections between the MIAS computer and the Bendix MLS 20-A receiver and its Control Display Unit (CDU) are described.

### F.1 MLS receiver connectors

In figure F.1, the Bendix MLS receiver is shown with its CDU. The MLS receiver has three connectors: two antenna connectors and one data connector. The connector types are listed in table F.1.

The receiver can be connected to two antenna's, one at the front of the aircraft and on at the tail. If only one antenna is used, the 'forward' connector should be used. In that case the 'aft' connector should be loaded with a 50 ohm resistor.

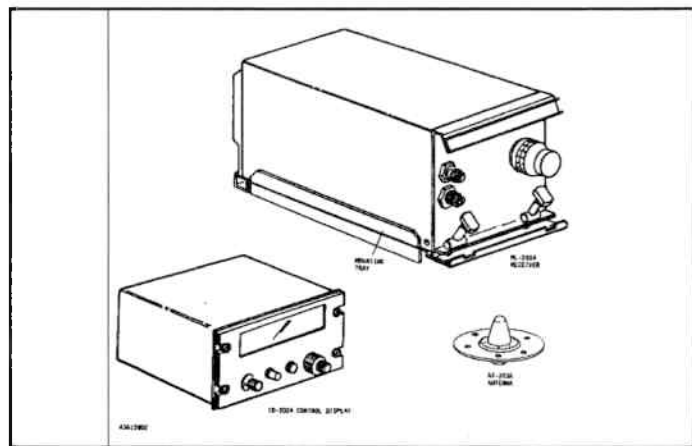


Figure F.1 MLS receiver, CDU and antenna

Table F.1 Bendix MLS-20A connectors

Unit	Connector	Name	Manufacturer
Receiver	J1	Mating connector	Cannon KPT06B24-61SZ
	J23 & J24	TNC Mating connectors	King KA-59-354M07
Control Display	J1	Mating connector	Positronic HDC25F20JVL or D-25 female

The data connector outputs data for driving different kinds of Course Deviation Indicators (CDI) and two digital serial data outputs, which characteristics are similar to ARINC 429 characteristics. These serial data outputs are connected to the MIAS computer. Furthermore, there are outputs for connection with the CDU and so called 'strap pins' which can be used to program minimum glideslope and Source Destination Indicators (SDI). There are also some outputs for testing.

The ARINC 429 data channel transmits azimuth and elevation angle information which is of interest. This angle information is not filtered. The MLS angle information which is used to drive a CDI is filtered though. The ARINC 429 labels for the angle functions are listed in table F.2. The

Table F.2 Bendix MLS-20A function labels in ARINC 429 output

Label (oct)	Word description	Field description	bits used
151	Approach Azimuth angle	Label	1-8
		SDI	9-10
		CTRL	11-12
		ANGLE DATA	13-29
		SSM	30-31
		PARITY	32
152	Approach Elevation angle	Label	1-8
		SDI	9-10
		CTRL	11-12
		ANGLE DATA	13-29
		SSM	30-31
		PARITY	32
340	Back Azimuth angle	Label	1-8
		SDI	9-10
		CTRL	11-12
		ANGLE DATA	13-29
		SSM	30-31
		PARITY	32

example of the ARINC 429 word coding in [18] is not correct. An example of correct coding is shown in figure F.6. The MLS receiver does not pas MLS data words on the ARINC channel.

The MLS DPSK data signals are transmitted on the 'MLS data' pins, and are decode using a separate device.

Figure F.2 shows the functions of the pins of all connectors of the MLS receiver and CDU. Figure F.5 shows the position of all pins on the connector that matches the data connector on the MLS receiver.

### E.1 MLS CDU connector and controls

The Control Display Unit (CDU) is used to control the MLS receiver and to display the status of the receiver. The CDU is connected to the MLS receiver using a 25 pin male D connector. The connections between the CDU connector and the MLS receiver connector are listed in figure F.2. The D connector was originally secured using braces, but this was changed to accommodate bolts.

The CDU controls are shown in figure F.3. Control nr 1 is the volume knob for the morse code which is transmitted by the MLS transmitter.

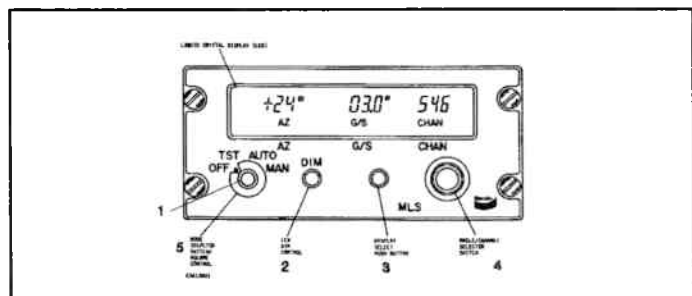


Figure F.2 MLS CDU controls



selects the value for the active parameter. The outer knob selects the most significant number, the inner knob the least significant number. Control nr 5 is the on/off knob. It also selects the operating mode.

More information about the Bendix MLS 20-A receiver can be found in the [18].

### *F.3 MLS to MIAS computer interface*

The MIAS computer will use the ARINC 429 like data stream and the MLS DPSK data stream.

To interface the MIAS computer with the ARINC 429 like data stream, an ARINC 429 interface board was bought. The M429PC board from MAX Technologie enables receiving and transmitting one ARINC 429 channel. The ARINC 429 channels are connected to the interface board using male D 25 connector. Figure F.4 shows the functions of the pins on the D connector that fits the M429PC board. This board can be programmed to various modes. Information about programming the board can be found in [16] and [15], table F.4 lists an example of how to use the M429PC board for receiving ARINC 429 data on line.

The MLS DPSK data is connected to the MIAS computer using a special device called B/ADW converter. The MLS DPSK data line transmits serial data at a rate of 15625 bits per second, using a bipolar return to zero coding. The B/ADW converter reads the bits and shifts them in a register. As soon as a preprogrammed bit pattern is recognised, the B/ADW converter interrupts the MIAS computer and the bits are read by the MIAS computer. The connection between the B/ADW

Table F.3 Connection between the MLS receiver and the B/ADW converter.

MLS connector pin number	MLS connector pin name	B/ADW converter pin number	B/ADW converter pin name
AA	MLS data	3	sin429
DD	MLS data return	2	gnd429
	not connected	1	shield

converter and the MLS receiver is listed in table F.3 using the pin number on both connectors.

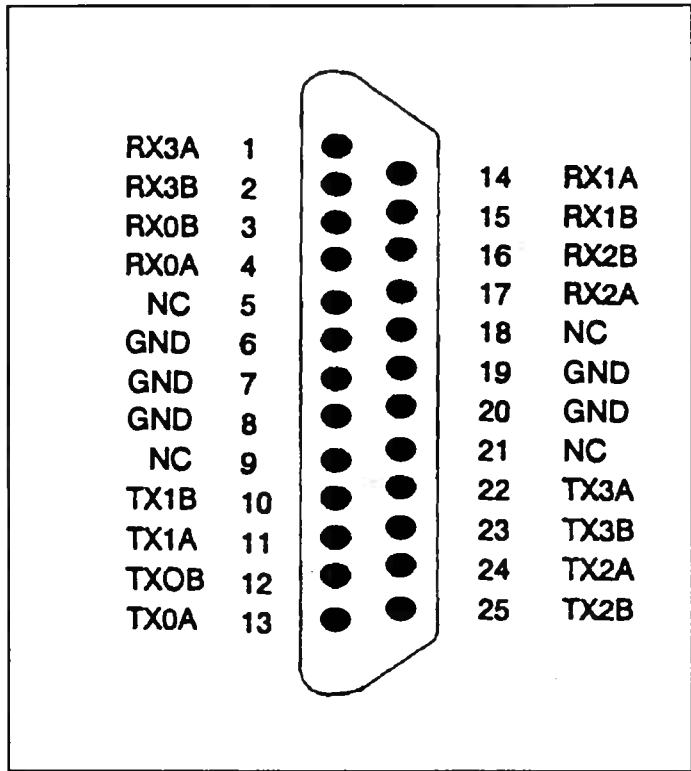


Figure F.4 ARINC 429-to-Computer connector

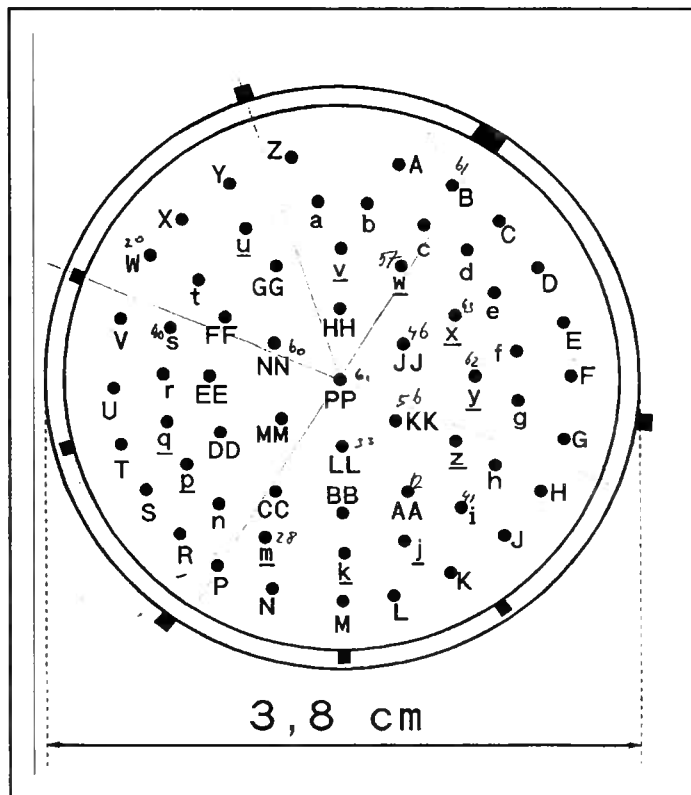


Figure F.5 MLS data-connector lay out

Table F.4 Example for programming the M429PC ARINC 429 interface.

```
Uses Lib429P; { Special library for the MAX429PC card}
***** Initialisation *****
SetSpeed( 0, Pspeed, Pgap); { set transmitter speed and gap between transmissions}
arTxSetParity( 0, Pnone); { set transmitter channel parity to none, to allow other data to
                           override}
arTxChannel := off; { INITIALISE RECEIVER}
arRxStop( 0); { stop receiver}
arRxSpeedHigh( 0); { set receiver on high speed}

For x:= 0 To num -1 Do { make label list}
  selecttable[ x]:= oct( selecttable[ x]);
arRxSelectSet( 0, @Selecttable, num); { select the labels to be read}

arRxConfigWrite( 0, circular, shared, 42, nosync, 0, 0, 0);
arRxStatTrig( 0); { configure the receiver and start the receiver}
ptr1:= arRxGetPtr( 0); { initialise the buffer pointer}
***** Reading *****
ptr2:= arRxGetPtr( 0); { get pointer in buffer}
While (ptr1 <> ptr2) Do { If words in buffer read the words from the buffer and put
                        them in a larger buffer}
  ptr1:= arRxBuffer( 0, ptr1, arinc429buffer[ inp], time);
  inp:= ( inp + 1 ) Mod max429buf;
***** Sending *****
If ( parity = Podd) { program the status mask for parity}
Then Pstatus:= $00
Else Pstatus:= $01;

Pstatus:= Pstatus Or $80; { program status mask for 'slot on'}
arTxSetdata( 0, nextfreeslot, Parincw); { put data in next free slot on the channel}
arTxSetRate( 0, nextfreeslot, Prate); { set the transmit rate for slot 0}
arTxSlotOn( 0, nextfreeslot); { enable slot 0}

arTxChannelOn( 0); { turn channel on}
***** Closing *****
arReset( 0); { turn off channel 0}
```

	P	SSM	Data field	CTRL	SDI	Label
bit no.	3 2	3 3 1 0	2 2 2 2 2 2 2 2 2 2 2 2 2 2 2 2 9 8 7 6 5 4 3 2 1 0 9 8 7 6 5 4 3	1 1 2 1	1 0 9	8 7 6 5 4 3 2 1
Example		1 1	1 1 1 1 1 0 0 0 1 0 1 0 1 0 0 0 0	1 0	0 0	0 1 1 0 1 0 0 1
notes	6	5	4	3	2	1

**Notes:**

- Label: Bits 1-8. Identifies the function to follow. Bit 1 is LSB. The example code -13.8°
 

<u>Function</u>	<u>Octal code</u>
Azimuth (High rate & Normal):	151
Elevation	152
Back Azimuth	340
- SDI (Source Destination Identifier): Bits 9 and 10.
 

<u>10</u>	<u>9</u>	<u>Installation no</u>	<u>10</u>	<u>9</u>	<u>Installation no</u>
0	0	All call	1	0	2
0	1	1	1	1	3
- Control: Bits 11 and 12
 

<u>Bit 11</u>	<u>Bit 12</u>
0 = Select Inhibit off	0 = Aft Antenna used this frame
1 = Select Inhibit on	1 = Forward Antenna used this frame
- Data field: Bits 13 - 29
 

<u>bit no</u>	<u>Definition</u>	<u>bit no</u>	<u>Definition</u>	<u>bit no</u>	<u>Definition</u>	<u>bit no</u>	<u>Definitio</u>
29	sign	24	10.24°	20	0.64°	16	0.04°
28	sign	23	5.12°	19	0.32°	15	0.02°
27	sign	22	2.56°	18	0.16°	14	0.01°
26	40.96°	23	1.28°	17	0.08°	13	0.005°
25	20.48°						

A right clearance indication is represented as a binary 'zero' in bit 29 and binary 'ones' in locations 13-28. A left clearance indication is the opposite. 'Zeros' in bits 27-29 locations indicates positive. 'Ones' indicate negative. When negative, the binary value of bits 13-26 should be calculated with bit 13 is LSB. Then 4000<sub>hex</sub> should be subtracted. The result multiplied with 0.005° is the indicated angle. When approaching an azimuth ground station, positive angles are to the pilots left, when approaching a back azimuth station, positive back azimuth angles are to the pilot's right. When approaching an elevation station, positive elevation angles are above the glide path.
- SSM (Sign Status Matrix): Bits 30 and 31
 

<u>31</u>	<u>30</u>	<u>Definition</u>	<u>Priority</u>	<u>31</u>	<u>30</u>	<u>Definition</u>	<u>Priority</u>
0	0	Failure Warn	1	1	0	Manual Self test	3
0	1	System flag	2	1	1	Normal operation	4
- Parity: Bit 32.  
Set to render Odd Parity.

Figure F.6 Example of the Bendix ARINC 429 coding.

## Appendix G The ARINC 429 protocol

In this section, the principle of the ARINC 429 data communication protocol is explained. First the use of ARINC 429 signals is treated, then the message structure and the electrical characteristics are described.

### G.1 ARINC 429 usage

The Aeronautical Radio Inc. (ARINC) is a corporation in which the United States scheduled airlines are the principal stockholders. An ARINC equipment characteristic is meant to standardize aircraft equipment so replacement is easy and cheap. Because the ARINC standards are relatively expensive to implement, the ARINC equipment is mainly used by larger aircrafts. General Aviation aircraft are usually equipped with more payable alternatives which sometimes resemble ARINC equipment.

The ARINC 429 characteristic defines a communication protocol for aircraft equipment. The ARINC 429 communication protocol is a serial data broadcast protocol which means that on one channel, only one transmitter may be connected. One channel can however be connected to one or more receivers. This way one sensor can be used by many systems. Figure G.1 shows this broadcast principle.

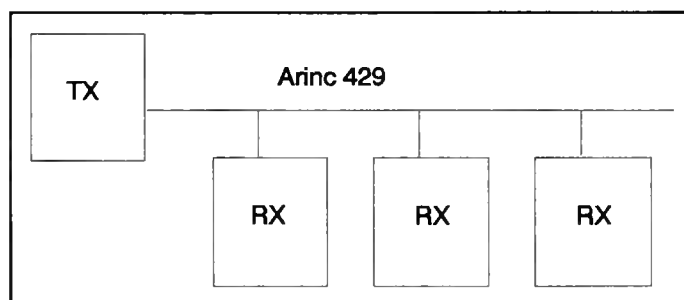


Figure G.1 ARINC 429 broadcast example

### G.2 Message structure

The ARINC 429 protocol defines messages. Each message consists of 32 bits, beginning with 8 label bits and ending with 1 parity bit. The rest of the bits can be used in a wide variety.

The label can represent 256 different messages. Every parameter of a device has its own label. The receivers can determine which parameter was transmitted by the number of the label and by the knowledge the receiver has about which device it is connected to. Depending on the label, the data bits in the message are treated differently. Table G.1 shows an example of the usage of ARINC 429 data bits for the ARINC 727 MLS receiver.

Table G.1 Examples of ARINC 429 function coding by the ARINC 727 MLS receiver. The ARINC 727 MLS receiver is defined in [6].

Label (oct)	Word description	Field description	bits used
130	MLS Auxiliary data group A part 1	Label	1-8
		SDI	9-10
		PADS	11-13
		DATA(I13-I28)	14-29
		SSM	30-31
		PARITY	32
131	MLS Auxiliary data group A part 2	Label	1-8
		SDI	9-10
		PADS	11-13
		DATA(I13-I28)	14-29
		SSM	30-31
		PARITY	32
132	MLS Auxiliary data group A part 3	Label	1-8
		SDI	9-10
		PADS	11-13
		Data (I45-I60)	14-29
		SSM	30-31
		PARITY	32
133	MLS Auxiliary data group A part 4	Label	1-8
		SDI	9-10
		MLS data link parity check	11
		Pads	12-13
		Data (I61-I76)	14-29
		SSM	30-31
		PARITY	32
164	MLS absolute glide path	Label	1-8
		SDI	9-10
		PADS	11-12
		Binary angle	13-27
		PAD	28
		Sign	29
		SSM	30-31
156	MLS basic data word 1	Label	1-8
		SDI	9-10
		PAD	11
		approach az to threshold dist	12-17
		approach az prop cov limit positive	18-22
		approach az prop cov limit negative	23-27
		Clearance signal	28
PAD	29		
SSM	30-31		
PARITY	32		

### G.3 Electrical characteristics

The ARINC 429 message is transmitted using a twisted shielded pair of wires. A digital one is transmitted by the A wire as +5 Volt pulse followed by a 0 Volt pause. This voltage is compared to the ground. The B wire transmits a one by putting a -5 Volt pulse on the wire at the same time as the

A wire pulses +5 Volt. It also pauses with 0 Volts. The differential voltage is therefore +10 Volts. To transmit a digital zero, the opposite is done compared to sending a one. This scheme is depicted in figure G.2.

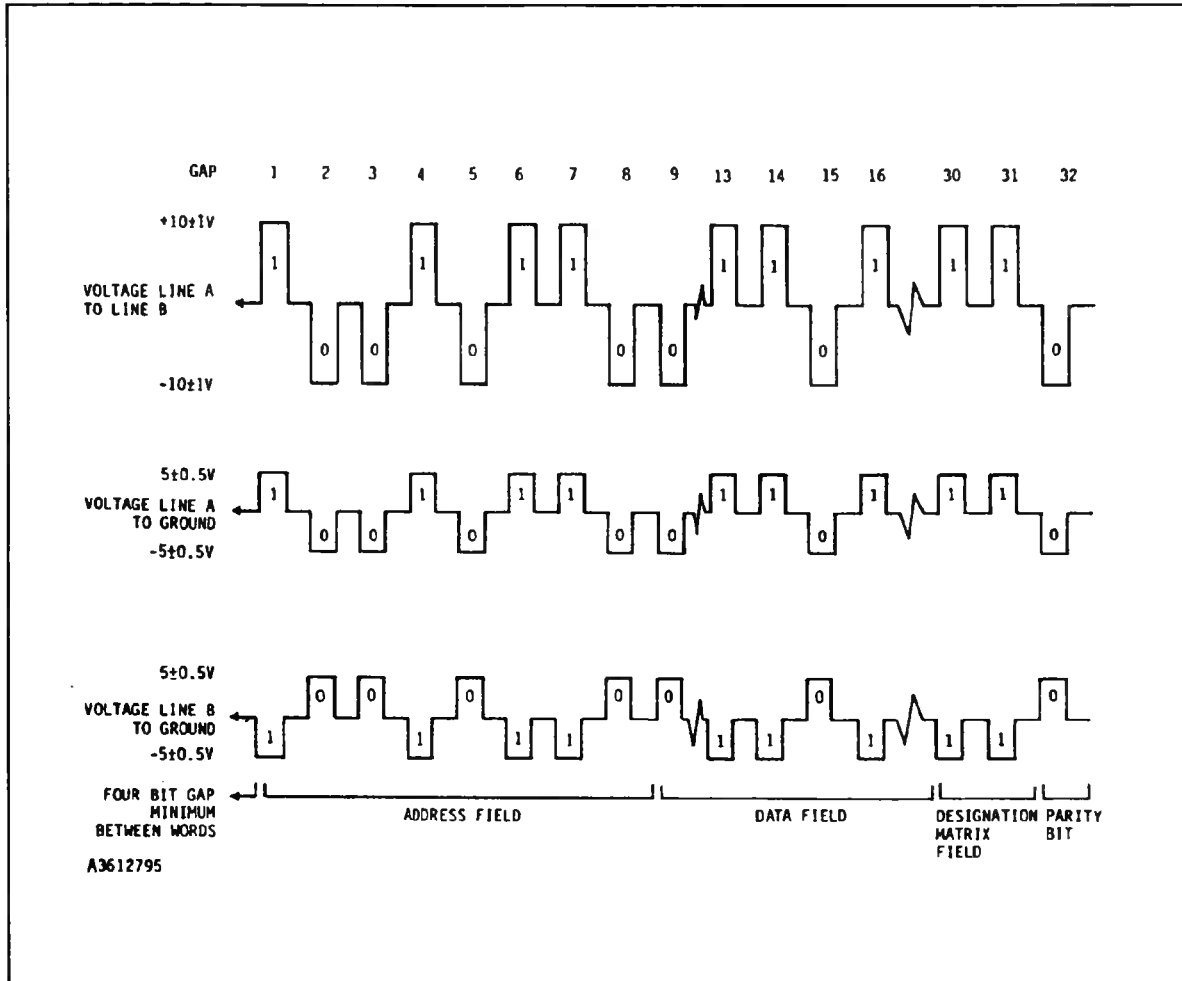


Figure G.2 Voltages of the ARINC 429 protocol

The width of the pulses are equal. The fast ARINC 429 protocol uses a 100 Kbit per second signalling rate. The slow version uses about 10 Kbit per second.

More detailed information about the ARINC 429 characteristics can be found in [5].

## Appendix H Converting synchro signals to digital words

This section describes what synchro's are used for, how they work and how their signals can be converted to digital words. Only the AC synchro is treated here. Other synchro's are treated in [1].

### H.1 Why synchro's are used

Aircraft sensors are usually not located near displays. In the case of angle sensors, the measured angle needs to be transmitted in some kind of form to the display in the cockpit. A synchro pair can be used to do this. A synchro pair consists of a synchro transmitter and a synchro receiver. The synchro transmitter is connected for example to a gyro and the synchro receiver is connected to the display. Using five wires, the measured angle is transmitted by the transmitter and displayed by the receiver.

### H.2 Synchro operation

In figure H.1 an abstracted view of a synchro is given. The rotor coil is connected to an AC voltage with fixed amplitude and frequency. The rotor coil is connected to the shaft of which the angle is to be measured. The stator coils are positioned around the centre of the synchro at equal angles of  $120^\circ$ . The stator coils pick up the magnetic field from the rotor, which gives them a voltage, depending on the angle of the rotor. The resulting voltages are listed in (H.1).

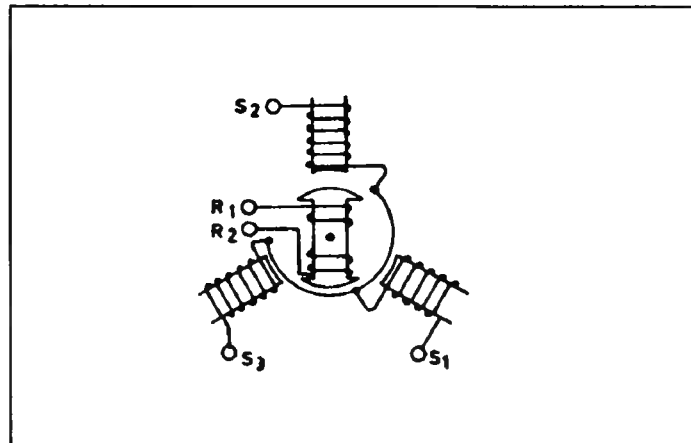


Figure H.1 Abstracted view of a synchro

$$\begin{aligned}
 V_{ref} &= V \cdot \sin(\omega t) \\
 V_1 &= V \cdot \cos(\theta) \cdot \sin(\omega t) \\
 V_2 &= V \cdot \cos\left(\theta + \frac{2\pi}{3}\right) \cdot \sin(\omega t) \\
 V_3 &= V \cdot \cos\left(\theta + \frac{4\pi}{3}\right) \cdot \sin(\omega t)
 \end{aligned}
 \tag{H.1}$$

Where  $\omega$  is the frequency of the AC voltage on the rotor in radians per second and  $\theta$  is the angle of the shaft in radians.

The generated voltages will form magnetic fields in the receiver synchro stator coils. If the rotor of the receiver synchro is connected to the same source as the rotor of the transmitter synchro the rotor of the receiver synchro will turn until it has the same angle as the transmitter synchro. Because the synchro transmitter and receiver function exactly the same, only their transmission or reception function distinguishes them from each other.

Synchro's can rotate a small load like a pointer. In most aircrafts, the amplitude of the AC voltage on the rotor is 26 Volts RMS at 400 Hz. The maximum amplitude on the stator coils is 11.8 Volts RMS.

### *H.3 Conversion of synchro signals to digital words*

To use the angle information in a digital computer, the angle information should be converted to binary words. As the angle is already coded with a synchro, it is logic to use the synchro signals and decode the angle information to a binary word.

Though it is possible to find the binary angle by sampling and quantising the synchro signals followed by some computation, another method is used. For industrial purposes several IC's have been developed to convert resolver signals, which are similar to synchro's signals, to binary words. The RDC-19220 is an example of a resolver to digital converters. It converts the angle to a binary word using a Phase Locked Loop (PLL) kind of structure. A counter contains the binary value of the angle. Three of these IC's have been combined on a single board, which can be plugged in one of the MIAS computer expansion slots. This board allows the conversion of three independent synchro signals to binary words. By putting the right address on the computer bus, one of the IC's will put its data on the data bus. Detailed information on this board and its design can be found in [25].